2016

# Cdk8 and Cdk19 as Novel Regulators of BMP4 Induced EMT in Cancer

Anne Elizabeth Serrao
*University of South Carolina*

Cdk8 and Cdk19 as Novel Regulators of BMP4 Induced EMT in Cancer

by

Anne Elizabeth Serrao

Bachelor of Arts
Washington & Jefferson College, 2013

---

Submitted in Partial Fulfillment of the Requirements

For the Degree of Master of Science in

Chemistry

College of Arts and Sciences

University of South Carolina

2016

Accepted by:

Mythreye Karthikeyan, Director of Thesis

Maksymilian Chruszcz, Reader

Lacy Ford, Senior Vice Provost and Dean of Graduate Studies

**Abstract**

Bone morphogenetic protein 2/4 (BMP2/4), members of the transforming growth factor β (Tgf-β) superfamily, play a dichotomous role in the progression of cancers through cell growth suppression and the enhancement of tumorigenesis in a variety of cancers. Cyclin dependent kinase 8 (CDK8), a protein kinase that regulates gene transcription, is involved in a variety of cancers including breast and pancreatic cancers as well as in mediating BMP2 signaling via its canonical Smad1 pathway. Our studies show that BMP4 induced EMT signals primarily though Smad1 and that Yap1, a transcriptional co-activator, is necessary for BMP4 induced EMT. Using a highly specific ATP competitive inhibitor of Cdk8 and its twin kinase Cdk19, Senexin B, we find that blocking the kinase activity of Cdk8/19 decreases BMP4 transcription of genes associated with EMT and inhibits BMP4 induced invasion. By separately reducing the expression of Cdk8 and Cdk19, we show for the first time that these kinases have both distinct and overlapping functions. Our findings suggest that Cdk8 and Cdk19, along with Yap1, are crucial for dictating BMP4/Smad1 responses during EMT and each of these factors could serve as a selective therapeutic target to block BMP4 signaling in cancer progression.

## Table of Contents

## List of Figures

## List of Abbreviations

ALK ..... Activin Receptor-like Kinase

BMP ..... Bone Morphogenetic Protein

BMPR..... Bone Morphogenetic Protein Receptor

CDK..... Cyclin Dependent Kinase

ECM ..... Extracellular Matrix

EMT..... Epithelial to Mesenchymal Transition

SnxB..... Senexin B

Tgf-β..... Transforming Growth Factor β

YAP ..... Yes-Associated Protein

## Chapter 1

## Introduction

Epithelial cancer cells from a primary tumor can become metastatic by undergoing epithelial to mesenchymal transition (EMT). Activation of EMT is characterized by a loss of markers, such as e-cadherin and cell-cell adhesions, and a gain in mesenchymal markers, such as the transcriptional markers Snail and Slug and changes in the cytoskeletal structure, which can lead to an invasive phenotype [1]. EMT induced invasion largely contributes to the advanced metastases of cancers [2, 3].

Bone morphogenetic proteins 2 and 4 (BMP2/4) share an 83% homology in amino acid sequence, and comprise the largest subgroup of the transforming growth factor beta (TGF-β) superfamily [4]. The role of TGF-β1 in EMT has been widely characterized, however, the role of BMP2/4, particularly BMP4, in EMT has been less studied [5]. BMP2/4 canonically signal through the Smad1/5/8 proteins, which form a complex with the co-Smad, Smad4, that translocate to the nucleus to regulate the transcription of target genes [6] [7]. BMP2/4 have also been shown to signal independently of the canonical Smad pathway, such as through Smad2/3, RhoA/ROCK, TAK1/p38, and PI3-kinase [7-10]. BMPs regulate a variety of processes, including differentiation, cell proliferation, and EMT during development [7, 11, 12]. The role of BMP4 during cancer progression, however, has been paradoxical, given that it can act as both a

tumor suppressor and a tumor promoter [13-16]. In breast cancer, increased BMP4 lead to a decrease in metastasis to lung and bone, as well as lower BMP4 levels have been associated with higher grade cancers [16]. On the other hand, BMP4 overexpression can lead to increased cell invasiveness and alterations in cell morphology characteristic of EMT in a variety of cancers, including ovarian, pancreatic, and colon cancers [13-15].

Cyclin dependent kinase 8 (Cdk8) is a protein kinase that is part of the Mediator complex and regulates gene transcription by its association with RNA polymerase II [17]. Cdk8 regulation of gene transcription has a role in tumor formation and has been established as an oncogene in various cancers, including pancreatic and colon cancers and melanoma [18-20]. Cdk8 has also been shown to increase proliferation, growth, and migration in breast cancer [21, 22]. Cdk8 is involved in agonist-induced linker phosphorylation, and the lack of agonist-induced linker phosphorylation has been shown to lead to decreased Smad1 transcriptional responses [23]. Despite Cdk8's emerging role in cancer and having a crucial role in Smad1 linker phosphorylation, its role in Smad1 dependent EMT has yet to be elucidated.

YAP (Yes-associated protein) is a transcriptional co-activator that enhances BMP signaling through its interaction with Smad1 [23, 24]. YAP has also been shown to contribute to EMT and promote metastasis in breast and colorectal cancer cells [25-27]. Smad1 linker phosphorylation by Cdk8 in the nucleus also involves the nuclear translocation of Yap and creates a binding site for and recruits Yap to the BMP activated Smad1 [23]. This interaction of Yap

with Smad1 enhances BMP-induced Smad1 gene expression responses of *Id1*, *Id2*, and *Id3* [23].

During cancer progression, the ECM can become remodeled and result in an increase in matrix stiffness [28, 29]. Because cellular function is controlled by its physical surroundings, this change in matrix has an effect on cell behavior, with a decreased ability to develop stress fibers and a change in gene expression [30, 31]. Similarly, cell stiffness is altered during cancer progression. During BMP induced EMT, cancer cells decrease in stiffness, leading to increased cell invasiveness [32]. Yap activity is affected by matrix rigidity, with a compliant matrix resulting in a decrease in Yap nuclear localization and Yap inactivation [33]. This link between BMP and YAP could play a crucial role in BMP induced EMT on varying substrate stiffness.

In this study we show that BMP4 induces EMT in ovarian (OvCa429), pancreatic (Panc1), and breast (Py2T) cancer cells through the reorganization of e-cadherin and actin, the up-regulation of Snail and Slug, and increased invasion. Additionally, we show that BMP4 induced EMT is dependent on Smad1. We show that EMT and Smad1 localization are both dependent on matrix rigidity, with a more compliant matrix resulting in decreased EMT and inhibition of Smad1 nuclear localization. We find that BMP4 enhances Yap nuclear translocation and Yap enhances Smad1 dependent BMP4 induced EMT and invasion. In addition, we find that a compliant matrix inhibits BMP4 induced Yap translocation. Moreover, we show that Cdk8/Cdk19 are required for the

recruitment of the Smad-Yap interaction and are critical for for BMP4 induced EMT and invasion.

## Chapter 2

## Results

*Matrix rigidity and mechanosensitive YAP1 dictate BMP4 induced EMT Smad1 dependent responses.*

We have recently demonstrated that BMP4 induced EMT alters cell stiffness properties and response to mechanical force [32]. To test the effects of matrix rigidity on BMP induced EMT, we used three cell line models—OvCa429 cells, Panc1 cells, and Py2T murine breast cancer cells—that underwent EMT in response to BMP4 based on alterations to E-cadherin localization (Figure 2.11A) and the actin cytoskeleton (Figure 2.11B), changes in the EMT- transcription factors (Figure 2.12C), and increased invasion in response to BMP4 (Figure 2.12D-E). Using these three cell lines we first examined cellular morphology on fibronectin conjugated polyacrylamide gels of elastic modulus 0.5kPa (soft), 8kPa (medium) (Methods), or glass (high stiffness). Consistent with prior studies on the role of rigidity on cellular phenotypes [34, 35], we find that all three cancer cell lines exhibited differences in morphology on the 8kPa (medium) substrate versus 0.5kPa soft substrates (Figure 2.1 A,B), with cells on the soft substrates being rounded and forming clusters, regardless of treatment. Alternatively, cells on the stiffer substrates displayed an elongated morphology and were spread out from one another upon BMP4 treatment, whereas without treatment the cells were closely adhered with

a more polygonal-like appearance. Additionally, cells on the substrates 8kPa showed similar morphology to cells cultured on plastic and/ or glass (data not shown).

To examine the changes associated with BMP4 induced EMT, we treated the cells on the different substrates and examined cell morphology using actin along with E-cadherin localization (Figure 2.1B Figure 2.2C). We find that OvCa429 and Panc1 cells treated with BMP4 for 5 and 3 days, respectively, on the 8kPa showed similar actin morphology and E-cadherin localization as cells cultured on glass for 5 and 3 days for OvCa429 and Panc1, respectively. (Figure 2.1B, Figure 2.2C and Figure 2.11A-B), while cells on the 0.5kPa substrates showed no change in actin morphology or E-cadherin localization. E- cadherin remained tightly localized around cell- cell junctions along with cortical actin (Figure 2.1B, Figure 2.2C), in contrast to on stiffer substrates where E-cadherin appeared more scattered and diffuse, along with actin showed significant stress fibers (Figure 2.11B, Figure 2.12C). To test if these changes were associated with rapid induction of EMT associated transcriptional factors Snail, Slug, and Zeb1, we treated the cells on the different substrates with BMP4 for 24 hours, after the cells were plated on the substrates for at least 12 hours. We find that each of the three cell lines upregulated a subset of the examined transcription factors (Snail: 11 fold, 14 fold, and 17 fold, Slug: 25 fold, 24 fold, and 10 fold for OvCa429, Panc1, and Py2T, respectively, and 5.5 fold and 6.5 fold for Zeb1 in Panc1 and Py2T, respectively) at 8Kpa (Figure 2.2D) at levels comparable to plastic (Figure 2.12C). Cells on soft 0.5kPa gels, altered their transcription levels

to significantly lesser extents, in response to BMP4, as compared to the 8kPa substrates (Figure 2.2D).

To examine if this was due to a defect in mounting a signaling response to BMP4 on 0.5Kpa gels, we examined if Smad1 activation was altered on the substrates with varying rigidities. Phosphorylation of Smad1 was determined by treating cells with exogenous BMP4 after allowing the cells to grow for 24 hours on the different substrates. No significant difference in Smad1 activation (Figure 2.3E) was observed on the substrates with different rigidities indicating that change in response was not at the level of signal reception. Since no significant change in Smad1 phosphorylation was observed, we tested if Smad1 nuclear translocation in response to BMP4 was altered on 0.5kPa soft substrates. We examined Smad1 and the co-Smad Smad4 localization by treating the cells with BMP4 on the 0.5kPa and 8kPa substrates. We find that both Smad1 and Smad4 were excluded from the nucleus in compliant gels (0.5Kpa) in all three models, while BMP4 induced Smad1 and Smad4 localization to the nucleus occurs robustly in more rigid substrates at the 1 hr time point (Figure 2.4F for Smad1 and Figure 2.13B for Smad4) and at longer time points as well (data not shown). These data suggest that lower transcriptional response to BMP4 on soft substrates may be due to reduced nuclear Smad localization.

Since BMP4 can activate both Smad1 and non-Smad pathways [7], we confirmed that cancer EMT in response to BMP4 was largely driven by a Smad1 mechanism in the cell lines used. We examined the effect of dorsomorphin, an inhibitor of the BMP receptors BMPR1A/R1B that blocks Smad1 phosphorylation

[36], and performed shRNA to Smad1 on BMP4 induced EMT. Dorsomorphin significantly reduced BMP4 induced increase in Snail and Slug transcript levels (Figure 2.13A) and two siRNA constructs (Figure 2.3A) (Methods) to Smad1 significantly reduced BMP4 induced Snail and Slug transcription and suppressed BMP4 induced cell invasion (Figure 2.3 B,C,D). While these data do not rule out possible contributions of non-Smad pathway or Smad2/3 involvement [7], they confirm Smad1's significant role in mediating BMP4 induced EMT in the different cancer cell line model systems and suggest that failure to mount a Smad1 response on substrates of 0.5kPa rigidity may lead to a failure to mount an EMT response as well.

To define the mechanistic impact of substrate rigidity on BMP4 induced EMT, we hypothesized a role for the mechanosensitive Yap1 [33] that besides being regulated by the Hippo pathway can also interact with Smad1 in a BMP dependent manner [23]. To test a direct role for Yap1, we used two independent shRNAs to Yap1 in the two human cell lines Panc1 and OvCa429 (Figure 2.5A). We find that BMP4 induced EMT transcription factors Snail and Slug, were suppressed 2.5 and 9 fold in OvCa429 and Panc1 shYap cells, respectively, compared to control cells (Figure 2.5B). Similarly, shYap1 reduced BMP4 induced cell invasion in OvCa429 and Panc1 cells by 10 and 14 fold, respectively (Figure 2.6C,D). These data implicate Yap1 in mediating BMP4 dependent EMT responses. Since Yap1 can integrate multiple signals including the Hippo pathway [37] and matrix rigidity [33], and is required for BMP4 induced EMT (Figure 2.5B, Figure 2.6D), we asked if BMP4 could induce nuclear translocation

of Yap1 to facilitate EMT. We find that BMP4 increases and induces the nuclear translocation of Yap1 on rigid substrates even in cells that have cell- cell contact (8kPa, Figure 2.6E). However, BMP4 does not increase the amount of Yap1 in the nucleus on soft substrates—where BMP4 was unable to induce EMT (Figure 2.6E). These Yap1 shRNA findings, together with a role for Smad1 in BMP4 mediated EMT reduction, suggest a role for nuclear Yap1 in mediating Smad1 induced EMT.

*The kinase activities of Cdk8 and Cdk19 are required for BMP4 induced EMT*

Our data strongly indicate that BMP4 induced EMT is driven by nuclear Smad1 and Yap1. However, Yap interaction with Smad1 and its ability to mediate Smad1 responses is dependent on the activity of the mediator kinase CDK8 in the nucleus that phosphorylates the Smad1 linker region resulting in recruitment of Yap1 [23]. Therefore, we tested a role for CDK8 in BMP4 induced EMT. To do this, we used the specific ATP competitive inhibitor of CDK8 and its isoform CDK19, Senexin B [38]. Inhibition of the kinase activity of the twin kinases CDK8/19 using Senexin B robustly suppressed BMP4 induced increase in the transcription factor Slug in OvCa429, Panc1, and Py2T EMT models and Snail and Zeb1 in Panc1 and Py2T cells without significantly altering baseline transcript levels (Figure 2.7A). Senexin B also lead to a suppression of BMP4 induced invasion in all three cell lines (Figure 2.8C,D and Figure 2.14A). Moreover this suppression was dose dependent (Figure 2.14 3A). Since our observation on substrates with different rigidities suggested a role for nuclear Yap1 in BMP4 induced EMT, and CDK8 dependent Smad1 linker

phosphorylation has been shown to be required for Yap interaction with Smad1 in the nucleus [23], we examined if blocking the kinase activity of CDK8/19 with Senexin B dampened BMP4 induced Yap nuclear translocation. Indeed, Senexin B treatment dampened Yap1 nuclear localization in response to BMP4 albeit to different extents in Py2T, Panc1, and OvCa429 cells (Figure 2.8B). These results demonstrate that the kinase activities of CDK8/19 that link Yap1 to Smad1 may be necessary for BMP4 induced EMT likely through the recruitment of Yap1 for mediating BMP4 induced EMT.

*Cdk8/Cdk19 are required for EMT.*

Since Senexin B targets the kinase activity of both CDK8 and CDK19, we asked if the effects of Senexin B were primarily due to CDK8, or if CDK19 could compensate for CDK8. To test the separate roles of CDK8 and CDK19, we reduced the expression of each CDK8 and CDK19 (Figure 2.9A) using 2 independent shRNA's for CDK8 and CDK19 (shRNA 1 to the coding region and shRNA2 to the 3' UTR region) were used in the studies. Reducing the expression of CDK8 and CDK19 individually reduced BMP4 induced Smad1 linker phosphorylation (Figure 2.9B) suggesting that both CDK8 and CDK19 could compensate for each other's loss. Consistent with the effects of Senexin B on reduced nuclear translocation of Yap1 in response to BMP4, reducing the expression of either CDK8 or CDK19 was able to suppress BMP4 induced Yap1 nuclear localization (Figure 2.9C) either due to alterations in retention of either Smad1 or Yap1 as previously proposed [23]. We next examined the effect of shRNA to Cdk8 and Cdk19 on BMP4 mediated increases in EMT transcriptional

factors Snail and Slug. We find that shRNA to CDK8 and CDK19 resulted in a suppression of BMP4 induced Snail and Slug in both Panc1 and OvC429 cells (Figure 2.9C, Figure 2.14B) (Figure 2.10D Panc1: shCdk8 1.5 and 3 fold, shCdk19 2.5 and 1.5 fold, Snail and Slug, respectively. Figure 2.14B OvCa429: shCdk8 2 fold and 2 fold, shCdk19 N.S. and 2 fold, Snail and Slug, respectively). These data indicate that while Cdk8 and Cdk19 have overlapping functions in mediating Smad1 linker phosphorylation (Figure 2.9B), they also have distinct functions in regulating transcription of individual genes. Finally, to examine if reducing Cdk8 and Cdk19 expression also impact BMP4 induced invasion in the different EMT models, we examined EMT induced invasion in OvCa429 and Panc1 cells. We find that while loss of Cdk8 did not affect baseline invasion (Figure 2.10F), shCdk8, reduced BMP4 induced invasion by 2 fold in both OvCa429 and Panc1 cells and shCdk19 reduced BMP4 induced invasion by 4 fold and 3 fold in OvCa429 and Panc1, respectively.

*Cdk8 and Cdk19 expression correlate with EMT genes in ovarian cancer*

Given that our *in vitro* studies indicate that *CDK8* and *CDK19* expression regulated EMT in ovarian cancer cell lines, we next assessed whether the expression of these genes correlated with common EMT markers in human high grade serous ovarian tumors. To address this question we examined RNAseq data from 283 high grade serous ovarian tumors (Data Not Shown) from the Cancer Genome Atlas (TCGA) project [39]. We first confirmed that positive correlations (Pearson) existed between up-regulated EMT markers. We found that *SNAI1*, *SNAI2*, *TWIST1*, *TWIST2*, *ZEB1*, and *ZEB2* each had a significant

positive correlation, ranging from 0.38 to 0.78, with the expression of each other EMT marker (data not shown). We further confirmed the significant negative correlation between *CDH1,* expression of which is lost during EMT*,* and *SNAI2*, *TWIST1* and *ZEB1*; *SNAI1*, *ZEB2*, and *TWIST2* were negatively correlated but only trended towards significance. Consistent with our *in vitro* results, expression of neither *CDK8* nor *CDK19* was negatively correlated with *CDH1.* However, *CDK8* expression had a significant positive correlation (Pearson Correlation: 0.14 – 0.24) with *SNAI1* (p=5.3E-04), *SNAI2* (p=5.2E-04), *ZEB1* (p=0.0051), *TWIST1* (p=0.0173), and *TWIST2* (p=5.1E-05) while CDK19 had a significant positive correlation (Pearson Correlation: 0.16 - 0.22) with *ZEB1* (p=2.0E-04) and *TWIST1* (p=0.0089). Coupled with our in vitro data, these results suggest that CDK8, and to a lesser extend CDK19, expression is significantly associated with EMT.

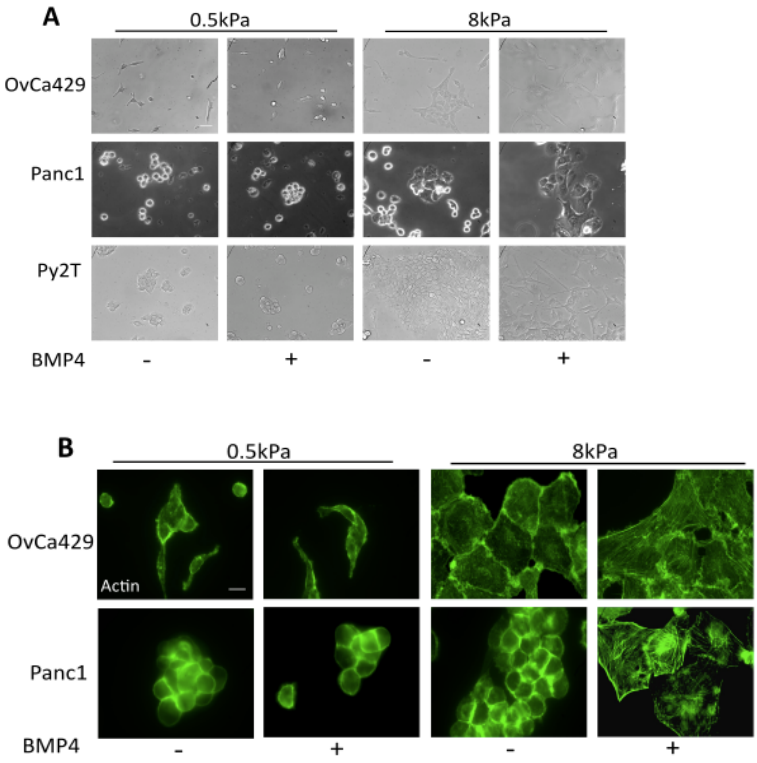


**Figure 2.1 BMP4 Induced EMT is Suppressed on Compliant Substrates.** (A) Phase contrast images of cells plated on soft (0.5kPa) and rigid (8kPa) fibronectin coated polyacrylamide (PA) hydrogels treated with BMP4 (10nM) for 5, 3, and 7 days, respectively. (B-C) Immunofluorescence images of OvCa429 and Panc1 cells plated on soft (0.5kPa) and rigid (8kPa) fibronectin coated PA hydrogels treated with BMP4 for 5 days and 3 days, respectively, followed by immunostaining with phalloidin for actin (B) and anti-e-cadherin.

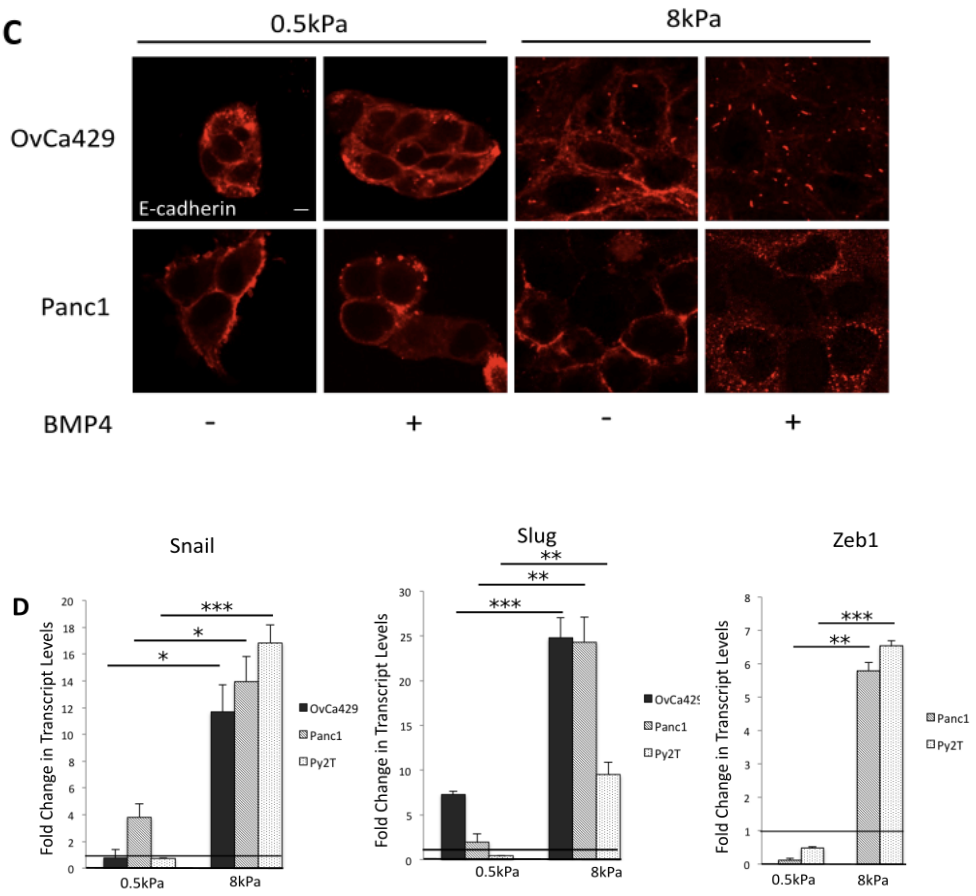


**Figure 2.2 (Figure 2.1 continued)** C) Scale bars 20μm. (D) Real time quantitative PCR showing the levels of the transcription factors Slug, Snail, and Zeb1 inOvCa429, Panc1, and Py2T cells plated on soft (0.5kPa) and rigid (8kPa) PA hydrogels treated with BMP4 for 5 days, 3 days, and 2 days, respectively. Values are normalized to their untreated control (black line). Graphs are representative of two independent experiments done in triplicate.*p<0.05, **p<0.01, *** p<0.001.

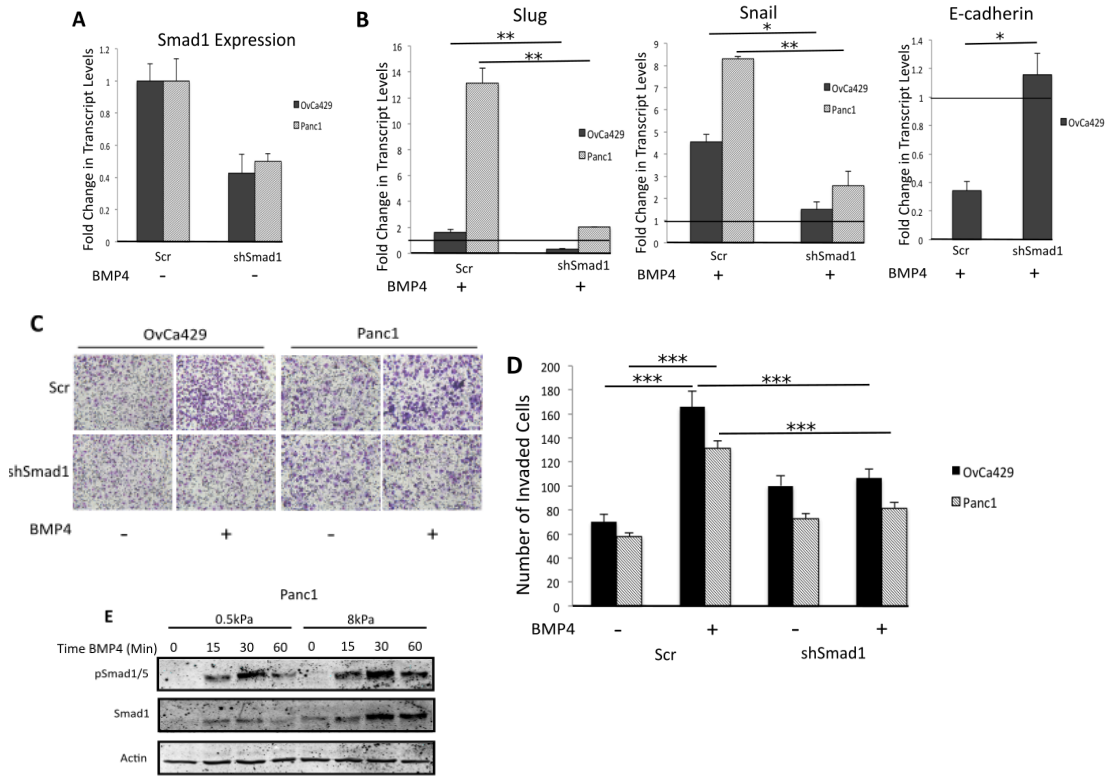


**Figure 2.3 BMP4 Induced EMT is Driven by Smad1** (A-B) Real time quantitative PCR showing expression fold change of Smad1 (A) and fold change in transcript levels, relative to the untreated control, for Slug, Snail, and E-cadherin (B) in OvCa429 and Panc1 cells expressing shSmad1 or shScr after being treated with BMP4 (10nM) for 24hrs and 12 hours, respectively. Values are normalized to their untreated control (Black horizontal bars). Error bars represent the standard error of the mean. *p<0.05, **p<0.01. (C-D) OvCa429 and Panc1 cells expressing shSmad1 or shScr cells were treated with BMP4 (10nM), then immediately plated in transwell chambers coated with MatriGel (400µg/mL). Cells were allowed to invade for 18 hours. Images (C) are cells on the underside of the chamber taken at x10. Images are representative of two independent experiments done in triplicate. Graphical representation of the number of invading cells from four independent fields. Error bars represent the standard error of the mean. *** p<0.001. (E) Time course of Smad1/5 phosphorylation in Panc1 cell lines treated with BMP4 (10nM) plated on soft (0.5kPa) and rigid (8kPa) fibronectin coated polyacrylamide (PA) hydrogels. Lysates were analyzed by immunoblotting with indicated antibodies.

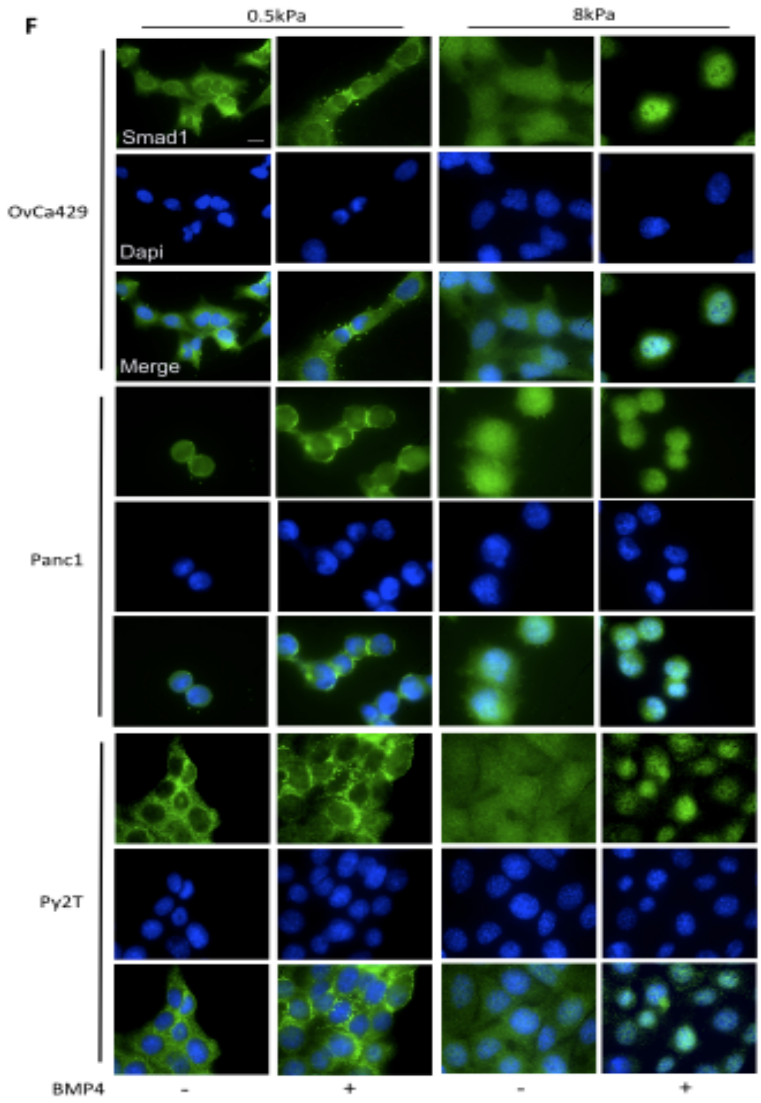


**Figure 2.4 Figure 2.3 Continued.** (F) Immunofluorescence images of OvCa429, Panc1, and Py2T cells plated on soft (0.5kPa) and rigid (8kPa) fibronectin coated PA hydrogels treated with BMP4 (10nM) for 1 hour, respectively, followed by immunostaining with anti-Smad1. Overlay images are shown with the nuclear stain 4', 6-diamidino-2-phenylindole. Scale bar = 20μm.

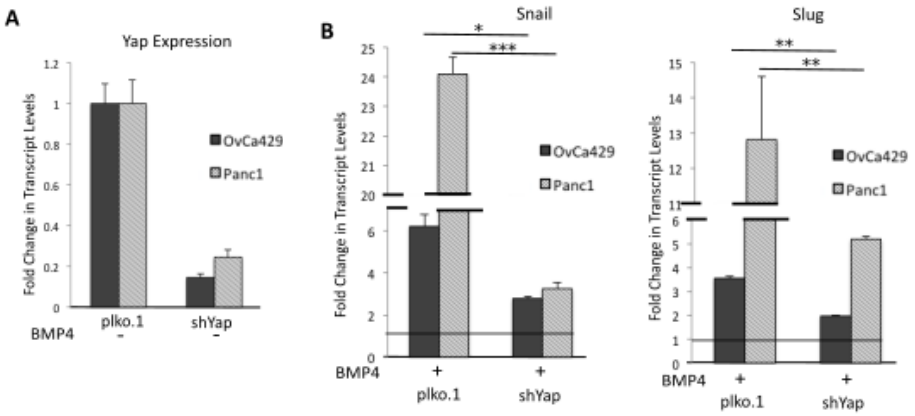


**Figure 2.5 Yap1 Enhances BMP4 Induced EMT.** (A-B) Real time quantitative PCR showing Yap1 fold changes in the knockdown cell lines as indicated (A) and the fold change of the transcription factors Snail and Slug in OvCa429 and Panc1 cells expressing shYap or shPlko1 after being treated with BMP4 (10nM) for 24hrs and 12hrs, respectively (B). Values are normalized to their untreated control (Black horizontal line) *p<0.05, **p<0.01, *** p<0.001.

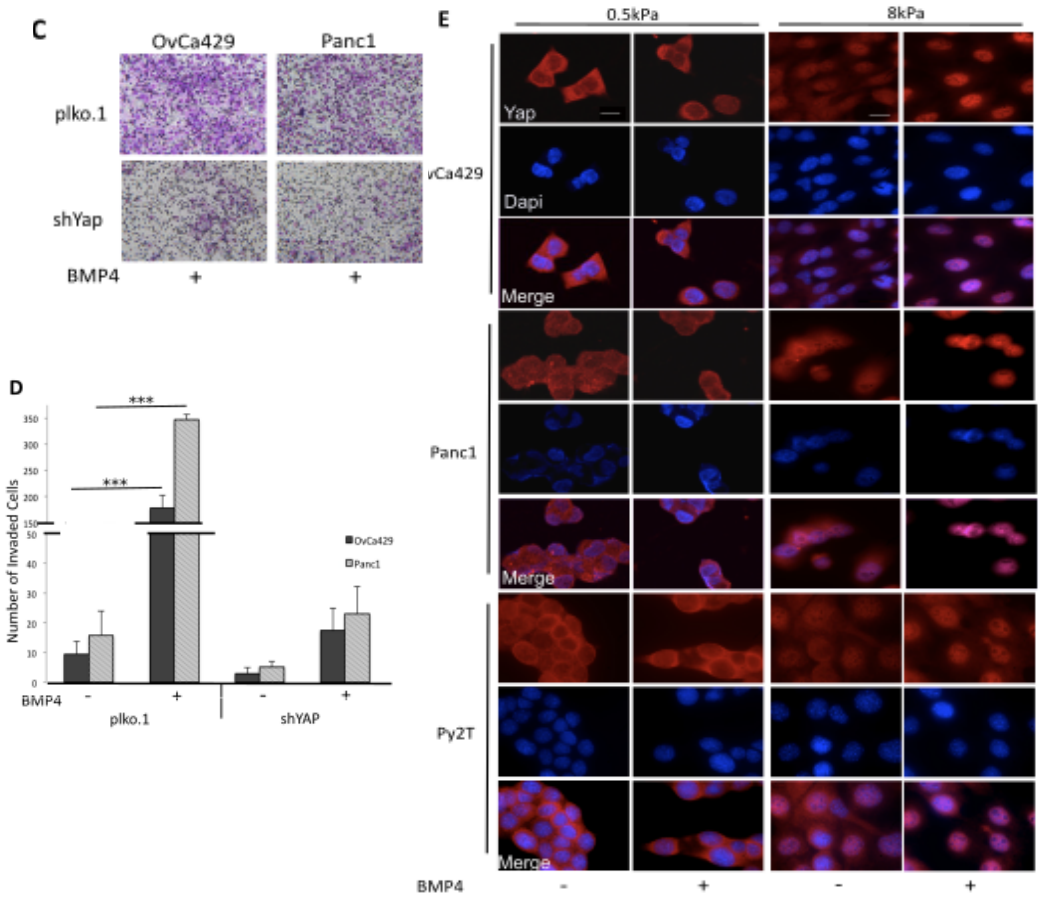


**Figure 2.6 Figure 2.5 continued.** (C-D) OvCa429 and Panc1 cells expressing shYap or shPlko1 were treated with BMP4 (10nM), then immediately plated in transwell chambers coated with MatriGel (400µg/mL). Cells were allowed to invade for 18 hours. (C) Images are cells on the underside of the chamber taken at x10. Graphical representation of the number of invading cells from four independent fields. Error bars represent the standard error of the mean (E) Immunofluorescence images of OvCa429, Panc1, and Py2T cells plated on soft (0.5kPa) and rigid (8kPa) fibronectin coated PA hydrogels treated with BMP4 (10nM) for 1 hour followed by immunostaining with anti-Yap. Scale bar = 20µm.

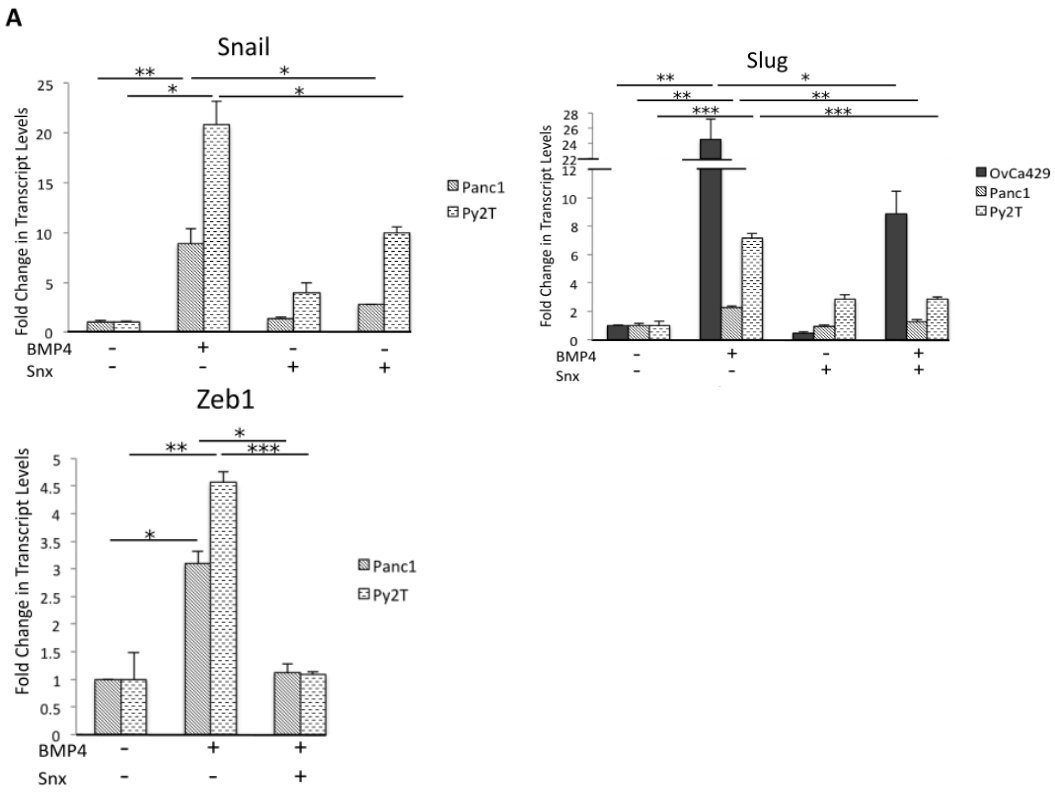


**Figure 2.7 The Kinase Activity of Cdk8/19 Enhances BMP4 Induced EMT.** (A) Real time quantitative PCR showing the fold change in levels of the transcription factors Snail, Slug, and Zeb1 inOvCa429, Panc1, and Py2T cells pre-treated with SnxB (5μM) for 30 minutes, then treated with BMP4 (10nM) for 24hrs, 12hrs, and 48hrs, respectively. Graphs are representative of two independent experiments done in triplicate. Error bars represent the standard error of the mean. *p<0.05, **p<0.01, *** p<0.001.

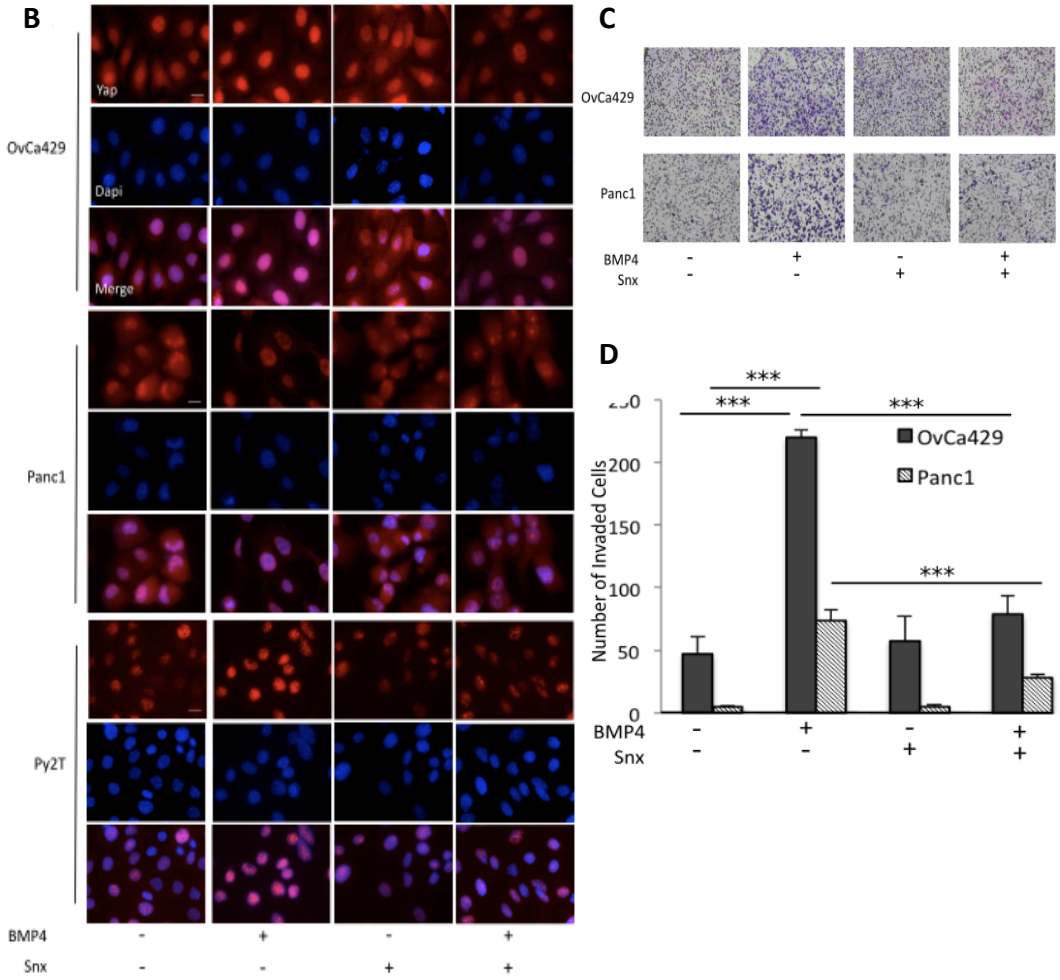


**Figure 2.8 Figure 2.7 continued.** (B) Immunofluorescence images of OvCa429, Panc1, and Py2T cells pre-treated for 30 minutes with SnxB (5μM), then treated with BMP4 (10nM) for 24 hours followed by immunostaining with Yap. Scale bars = 20μm (C) OvCa429 and Panc1 cells were pre-treated with SnxB (5μM) for 30 minutes, then treated with BMP4 (10nM), and then immediately plated in transwell chambers coated with MatriGel (400μg/mL). Cells were allowed to invade for 18 hours. Graphical representation of the number of invading cells from four independent fields. Error bars represent the standard error of the mean.

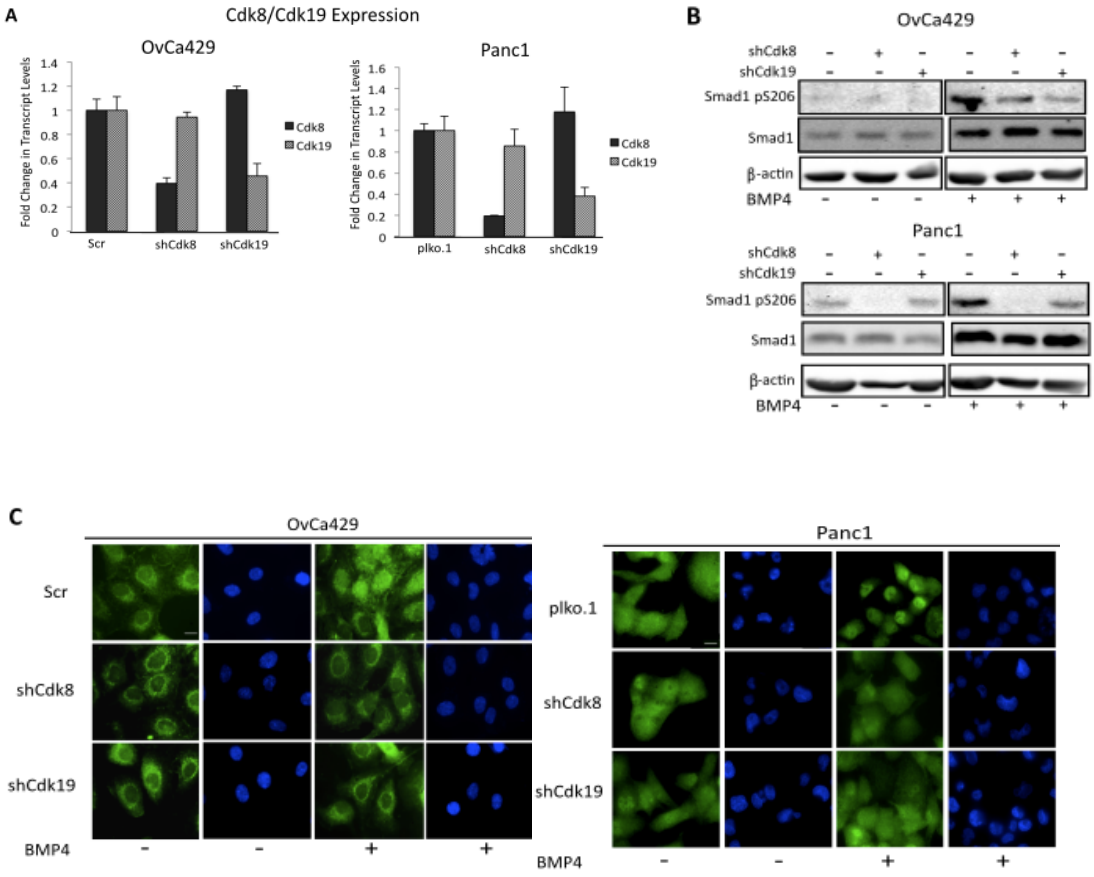


**Figure 2.9 Cdk8/19 Enhance BMP4 EMT and Exhibit Differential Effects.** (A) Real time quantitative PCR showing the levels of Cdk8 and Cdk19 in OvCa429 and Panc1 cells. (B) OvCa429 and Panc1 cells with stable shRNA Cdk8 and Cdk19 knockdown were treated with BMP4 (10nM) for 1 hour, analyzed by immunoblotting with the indicated antibodies. (C) Immunofluorescence images of OvCa429 and Panc1 cells expressing shScr, shplko.1, shCdk8, or shCdk19 treated with BMP4 for 24 hours, followed by immunostaining with anti- Yap. Scale bar = 20μm.

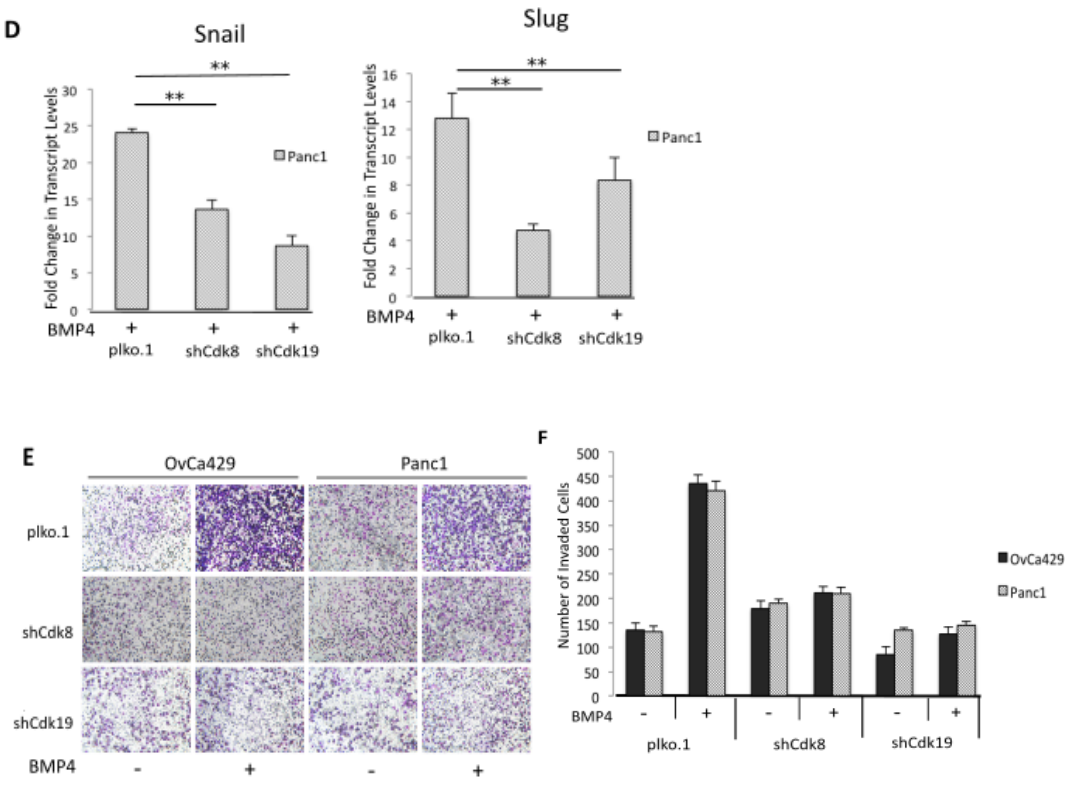


**Figure 2.10 Figure 2.9 Continued** (D) Real time quantitative PCR showing the levels of the transcription factors Snail and Slug in Panc1 cells expressing shPlko.1, shCdk8, or shCdk19 treated with BMP4 (10nM) for 24 hours. Graphs are representative of two independent experiments done in triplicate. Error bars represent the standard error of the mean. *p<0.05, **p<0.01, *** p<0.001. (E-F) OvCa429 and Panc1 cells were treated with BMP4 (10nM), then immediately plated in transwell chambers coated with MatriGel (400µg/mL). Cells were allowed to invade for 18 hours. (E) Images are cells on the underside of the chamber taken at x10. Images are representative of two independent experiments done in triplicate. (F) Graphical representation of the number of invading cells from four independent fields. Error bars represent the standard error of the mean.

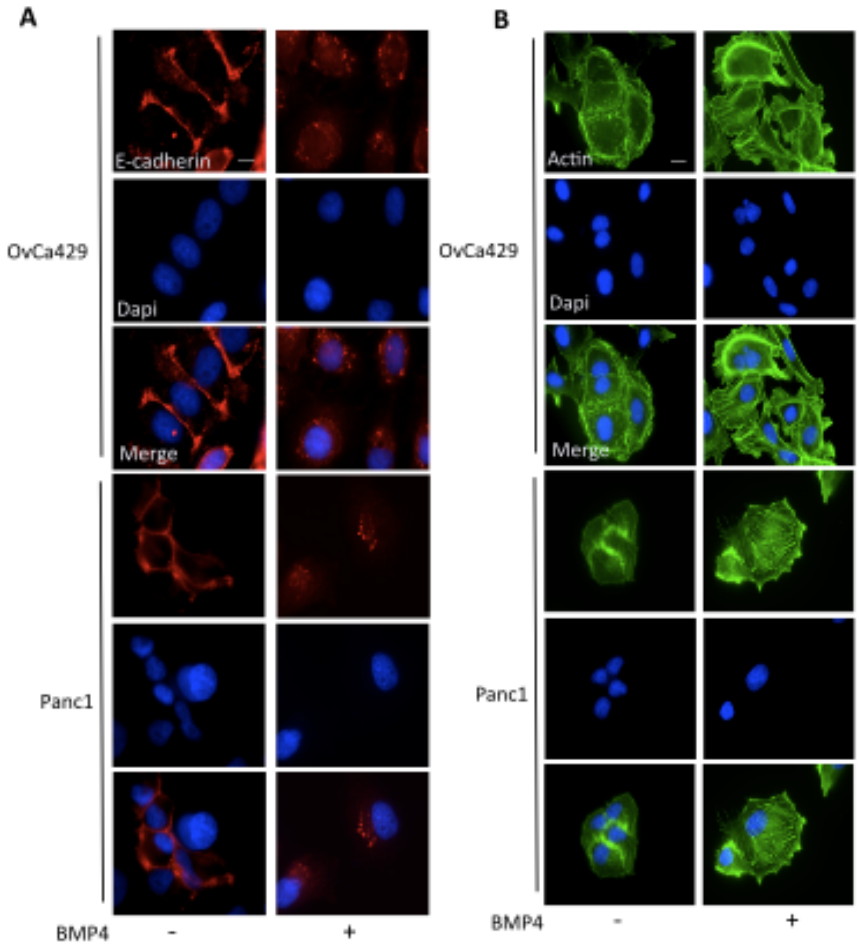


**Figure 2.11. Supplementary Figure 1**. (A) OvCa429 and Panc1 cells treated with BMP4 (10nM) for indicated times. Lysates were analyzed by immunoblotting with indicated antibodies. (B) OvCa429 and Panc1 cells treated with BMP4 (10nM) for 5 and 3 days, respectively, followed by immunostaining with anti-E-cadherin or phalloidin for actin. Scale bars = 20μm. Done in triplicate. Error bars represent the standard error of the mean.

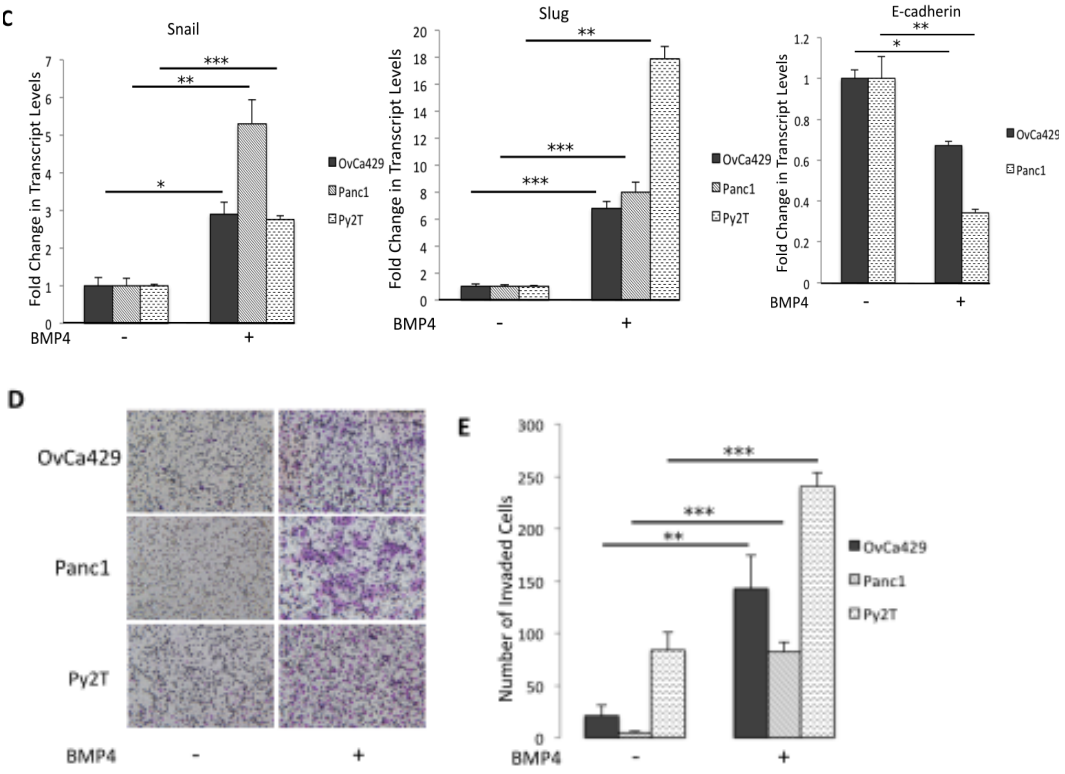


**Figure 2.12 (Figure 2.11 Supplementary Fig 1 continued):** (C) Real time quantitative PCR showing the levels of the transcription factors Snail, Slug, and E-cadherin in OvCa429 and Panc1 cells treated with BMP4 (10nM) for 24 and 12 hours, respectively. Graphs are representative of two independent experiments (D-E) OvCa429 and Panc1 cells were treated with BMP4 (10nM), then immediately plated in transwell chambers coated with MatriGel (1mg/mL). Cells were allowed to invade for 2 days. Images (B) are cells on the underside of the chamber taken at x10. Images are representative of two independent experiments done in triplicate. Graphical representation of the number of invading cells from four independent fields. Error bars represent the standard error of the mean.

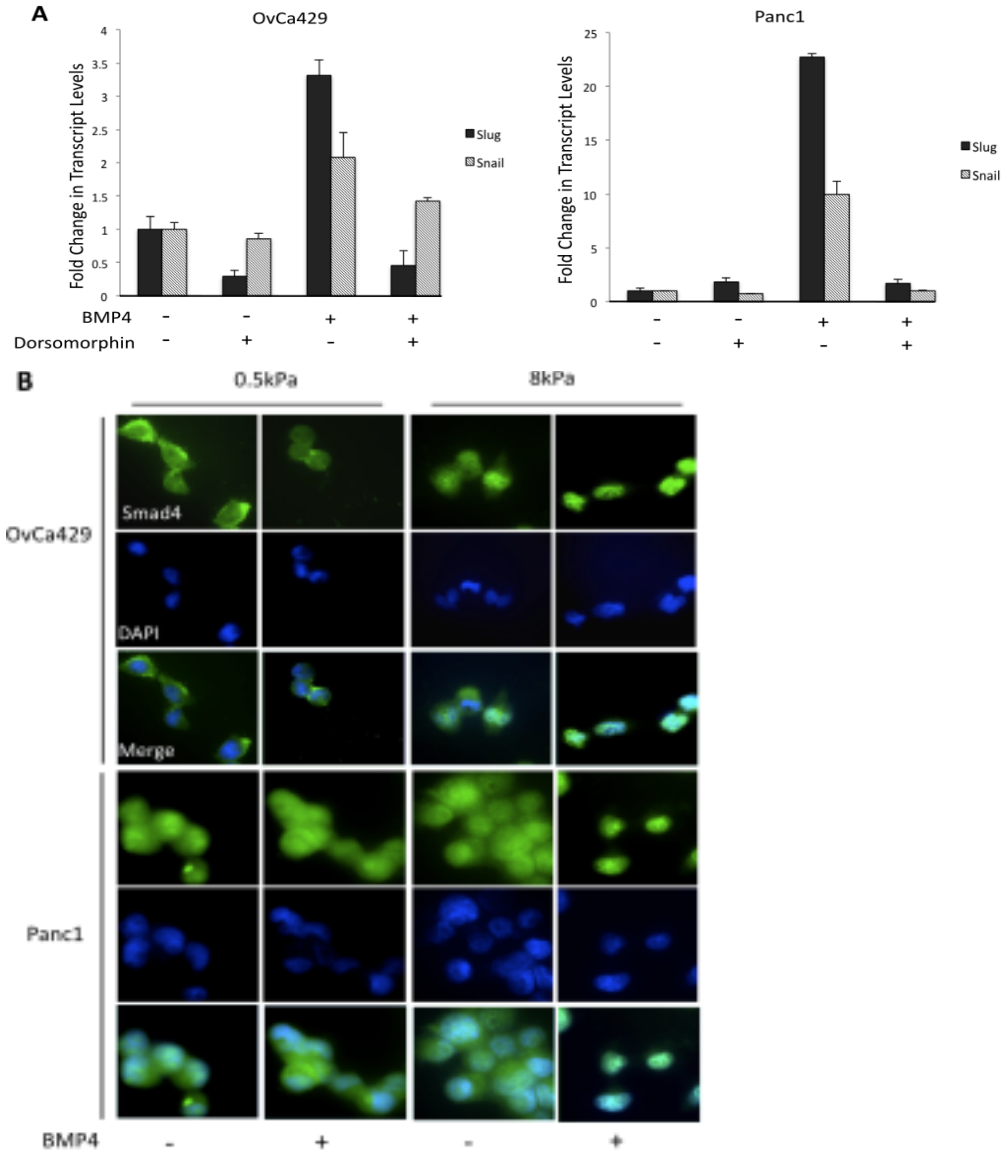


**Figure 2.13. Supplementary Figure 2** (A) Real time quantitative PCR showing the levels of the transcription factors Snail and Slug in OvCa429 and Panc1 cells pre-treated with dorsomorphin (5μM) for 30 minutes, then treated with BMP4 (10nM) for 24 and 12 hours, respectively. (B) Immunofluorescence images of OvCa429 and Panc1 cells plated on soft (0.5kPa) and rigid (8kPa) fibronectin coated PA hydrogels treated with BMP4 (10nM) for 1 hour, respectively, followed by immunostaining with anti-Smad4. Overlay images are shown with the nuclear stain 4',6-diamidino-2-phenylindole.

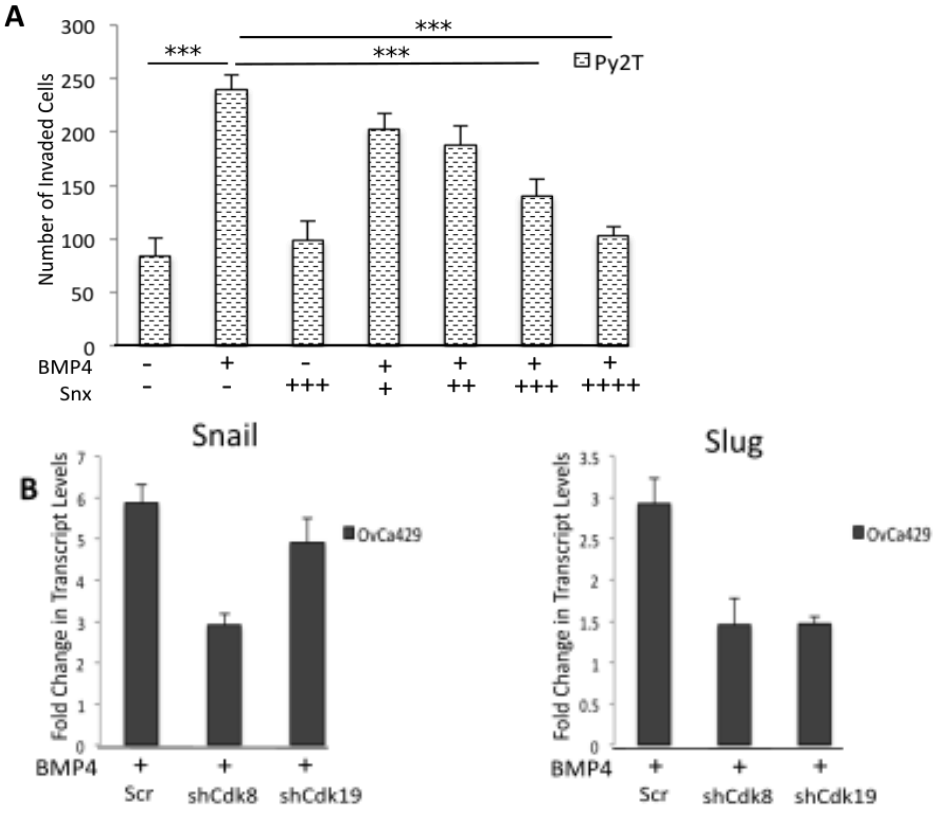


**Figure 2.14. Supplementary Figure 3** (A) OvCa429 and Panc1 cells were pre-treated with SnxB with increasing concentrations from 250nM, 500nM, 1μM, and 5μM for 30 minutes, then treated with BMP4 (10nM), and then immediately plated in transwell chambers coated with MatriGel (400μg/mL). Cells were allowed to invade for 18 hours. Error bars represent the standard error of the mean. (B) Real time quantitative PCR showing the levels of the transcription factors Snail and Slug in OvCa429 cells expressing shScr, shCdk8, or shCdk19 treated with BMP4 (10nM) for 24 hours. Graphs are representative of two independent experiments done in triplicate. Error bars represent the standard error of the mean.

## Chapter 3

## Discussion

The role of BMP4 in the progression of cancer has been conflicting given that it has been shown to increase cell invasiveness, migration, and metastasis in some cancers [13-15, 40], however, has been shown to suppress growth and found in lower levels in other cancers [16, 41]. Determining the signaling pathway and specific factors involved in BMP4 induced EMT could help identify under what conditions BMP4 acts as a tumor suppressor or promoter. Previous studies have shown that BMP4 is able to signal through Smad1 and Smad2 [7]. Our studies confirm that BMP4 induced Smad1 activation prompts EMT in ovarian, pancreatic, and breast cancer cell models (Figure 2.3B-D, Fig 2.13). The present study shows the requirement of the transcriptional regulators Cdk8/19, as well as the transcriptional co-activator Yap1 in Smad1 dependent BMP4 induced EMT in ovarian, pancreatic, and breast cancer cell line models. We also find that Yap1, Cdk8, and Cdk19 are each responsible for the increases in the EMT associated transcription factors Snail and Slug along with the increase in cell invasion associated with BMP4 signaling. Consistent with previous studies, our data show that Cdk8 is necessary for the linker phosphorylation of Smad1 [23], along with its isoform Cdk19. The ability of both Cdk8 and Cdk19 to suppress BMP4 induced Snail, Slug, invasion, Yap1 nuclear retention, and Smad1 linker phosphorylation indicate not only that they are important in the

regulation of BMP4 induced EMT, but they may be able to compensate for one another.

Our study shows for the first time the use of Senexin B, the specific small molecule inhibitor of Cdk8 and Cdk19, in the involvement of suppressing transcriptional activation of EMT transcription factors Snail and Slug with robust effects on suppressing cell invasion, thus further confirming the role of Cdk8 and Cdk19 involvement in BMP4 induced EMT. These findings on the effects of Senexin B also have broader implications for the use of Senexin B as a potential therapeutic strategy for suppressing metastasis. Cdk8 has been shown to be an oncogene and leads to cancer progression in a variety of cancers including pancreatic, colon, and breast cancers and melanoma [18-22]. In addition to the BMP4/Smad1 signaling pathway, Cdk8 has also been shown to be involved in other signaling pathways, including Wnt/β-catenin, Tgf-β, and Notch [18, 23, 42]. The diverse role of Cdk8 indicates that Senexin B may be able to be used as a selective approach to improve cancer treatment.

We find that softer substrates dampen the effects of BMP4 on the EMT associated transcription factors, Snail and Slug, along with inhibiting E-cadherin dislocation from the junctions. This is similar to previous studies on matrix rigidity with Tgfβ−1, where decreased matrix rigidity reduced the levels of Tgfβ−1 induced Snail expression, as well as increasing E-cadherin localization along the cell junctions [34]. Since BMP4 induced EMT seems to be primarily driven by Smad1 (Figure 2B-D), this decrease in EMT response could be due to the exclusion of Smad1 and Smad4 from the nucleus. Prior studies on matrix

stiffness have shown that a decreased rigidity resulted in Yap exclusion from the nucleus [33]. In addition to Yap exclusion from the nucleus with softer substrates, we found that BMP4 is unable to override the mechanical control on Yap1, as Yap1 remains excluded from the nucleus on soft substrates. Cdk8/19, however, remained localized in the nucleus regardless of matrix rigidity (data not shown). Because matrix rigidity reduced the effects of EMT, while inhibiting Smad1 and Yap1 activity, this data could suggest that Smad1 and Yap1 are necessary for the activity of Cdk8/19 during BMP4 induced EMT. The particular mechanism by which Cdk8/19, Yap1, and Smad1 interact to drive BMP4 induced EMT had yet to be established. Future studies to examine the interplay among these factors will help elucidate their roles in the regulation of EMT by Cdk8/19.

## Chapter 4

## Materials and Methods

### Cell Lines and Culture Conditions

OvCa429 cells were obtained from Duke Gynecology/Oncology Bank, Panc1 cells were from ATCC, and Py2T cells were a kind gift from Gerhard Christofori (University of Basel). Panc1 and Py2T cells were cultured in DMEM containing L-glutamine, 10% fetal bovine serum (FBS), and 100 U of penicillin-streptomycin. OvCa429 cells were cultured in RPMI containing L-glutamine, 10% fetal bovine serum (FBS), and 100 U of penicillin-streptomycin.

### Softwells

For rigidity experiments, cells were plated on 0.5kPa (soft) or 8kPa (rigid) substrates (Matrigen, Softslip 12 well and Softwell 6 well) that were coated with 10ug/mL fibronectin (Cultrex® #3420-001-01) in 1X PBS for one hour. All cells were allowed to sit on substrates for at least 12 hours before BMP4 treatment.

For Smad1 (1 hour treatment) and Yap1 (24 hour treatment) localization experiments on Softslip 12 well, 50000 cells were plated on 8kPa substrates and 100000 cells were plated on 0.5kPa substrates. For E-cadherin and actin staining, plated 40000 cells on 8kPa and 80000 cells on 0.5kPa, 30000 cells on 8kPa and 60000 cells on 0.5kPa, and 10000 cells on 8kPa and 40000 cells on 0.5kPa for Panc1(3 day treatment), OvCa429 (5 day treatment with re-treatment at day 3), and Py2T cells(7 day treatment with re-treatment at day 4),

respectively. For time course experiments on Softwell 6 well, 200000 cells were plated on 8kPa substrates and 300000 cells were plated on 0.5kPa substrates. For qPCR experiments on Softwell 6 well, plated 50000 on 8kPa and 200000 cells on 0.5kPa for OvCa429 cells (5 day treatment with re-treatment at day 3), 80000 on 8kPa and 200000 cells on 0.5kPa for Panc1 cells (3 day treatment), and 70000 cells on 8kPa and 200000 cells on 0.5kPa for Py2T cells (2 day treatment).

**Antibodies, Reagents, Plasmids, and Lentiviral Infections**

Antibody E-cadherin (BD Biosciences #610181), B-Actin (Sigma #A2228) was from Sigma. pSmad1 Ser206 (#5753), pSmad1/5/8 (#9511), Smad1 (#6944), and Smad4 (#9515) antibodies were from Cell Signaling. Senexin B was from Senex. For Smad1 knockdown, OvCa429 and Panc1 cells were infected with 100MOI siRNA adenovirus construct, generously provided by Maria Trojanowska. Lipofectamine 2000 (Life Technologies #11668019). Constructs with the shRNA to Yap was obtained from Sigma with the following sequences: Yap:0000107265: CCGGCCCAGTTAAATGTTCACCAATCTCGAGATTGGTGAACATTTAACTGGG TTTTTG and Yap:0000107268:CCGGGACCAATAGCTCAGATCCTTTCTCGAGAAAGGATCT GAGCTATTGGTCTTTTTG. For Yap knockdown, OvCa429 and Panc1 cells were infected at a 1:8 ratio of the Yap shRNA lentiviral construct. The target sequences for Cdk8 shRNA were CCTCTGGCATATAATCAAGTT, and for Cdk19 was GCTTGTAGAGAGATTGCACTT. For Cdk8 and Cdk19 knockdown,

OvCa429 and Panc1 cells were infected at a 1:4 ratio of the Cdk8 and Cdk19 shRNA lentiviral construct. OvCa429 and Panc1 cells were selected in puromycin at 3μg and 5μg, respectively. All shRNA lentiviral constructs were generously provided by Serena Altilia (University of South Carolina). The knockdown was confirmed by qPCR (sequences in Table 1).

**Quantitative Polymerase Chain Reaction**

Panc1, OvCa429, and Py2T cells were treated for 12, 24, and 48 hours, respectively. In experiments where SenexinB was used, cells were pre-treated with SenexinB for 30 minutes. Total RNA was isolated from cells using Trizol reagent (Invitrogen, Carlsbad, CA). 1ug of RNA was reverse transcribed to cDNA using 5x iScript Reverse Transcription Supermix (Bio-Rad #1708840) and the Sso Advanced Universal SYBR Green Supermix (Bio-Rad #1725271). qRT-PCR primer sequences are listed in Table 1.

**MatriGel Invasion Assays**

Invasion assays were performed using 24-well transwells (Greiner Bio-One; ThinCerts™, 24 well 8.0um) coated with 400ug/ml MatriGel (BD Biosciences #3248404). Cells (50,000) in serum free media were plated in upper chamber, and allowed to invade for 18 hours toward serum media in lower chamber. Filters were stained with Three Step Stain (Richard-Allan Scientific). The filters were removed and mounted onto glass slides. Cells on the filter were counted using an Olympus DP21 microscope at x10 magnification.

**Immunofluorescence**

In experiments where SenexinB was used, cells were pre-treated with SenexinB for 30 minutes. Cells were fixed in 4% paraformaldehyde, permeabilized in 0.1% TX-100, and blocked with 1% BSA PBS. Cells were incubated in primary antibody (1:200) for an hour, followed by incubation with Alexa Fluor 488 or 594 second antibody (LifeTechnologies). After washing, cells were stained with 4'6-diamidino-2-phenylindole (Roche). Imaging was performed using an Olympus IX81 motorized inverted microscope. Imaging was performed using Imaging on substrates was performed using a Zeiss LSM700 confocal microscope.

## References


1. Kalluri, R. and R.A. Weinberg, *The basics of epithelial-mesenchymal transition.* J Clin Invest, 2009. **119**(6): p. 1420-8.
2. Lengyel, E., *Ovarian cancer development and metastasis.* Am J Pathol, 2010. **177**(3): p. 1053-64.
3. Li, D., et al., *Pancreatic cancer.* Lancet, 2004. **363**(9414): p. 1049-57.
4. Kawabata, M., T. Imamura, and K. Miyazono, *Signal transduction by bone morphogenetic proteins.* Cytokine Growth Factor Rev, 1998. **9**(1): p. 49-61.
5. Lamouille, S., J. Xu, and R. Derynck, *Molecular mechanisms of epithelial-mesenchymal transition.* Nat Rev Mol Cell Biol, 2014. **15**(3): p. 178-96.
6. Ross, S. and C.S. Hill, *How the Smads regulate transcription.* Int J Biochem Cell Biol, 2008. **40**(3): p. 383-408.
7. Holtzhausen, A., et al., *Novel bone morphogenetic protein signaling through Smad2 and Smad3 to regulate cancer progression and development.* FASEB J, 2013.
8. Wang, Y.K., et al., *Bone morphogenetic protein-2-induced signaling and osteogenesis is regulated by cell shape, RhoA/ROCK, and cytoskeletal tension.* Stem Cells Dev, 2012. **21**(7): p. 1176-86.
9. Pal, A., et al., *CCN6 modulates BMP signaling via the Smad-independent TAK1/p38 pathway, acting to suppress metastasis of breast cancer.* Cancer Res, 2012. **72**(18): p. 4818-28.
10. Gamell, C., et al., *BMP2 induction of actin cytoskeleton reorganization and cell migration requires PI3-kinase and Cdc42 activity.* J Cell Sci, 2008. **121**(Pt 23): p. 3960-70.
11. Richter, A., et al., *BMP4 promotes EMT and mesodermal commitment in human embryonic stem cells via SLUG and MSX2.* Stem Cells, 2014. **32**(3): p. 636-48.
12. Wang, R.N., et al., *Bone Morphogenetic Protein (BMP) signaling in development and human diseases.* Genes Dis, 2014. **1**(1): p. 87-105.
13. Theriault, B.L., et al., *BMP4 induces EMT and Rho GTPase activation in human ovarian cancer cells.* Carcinogenesis, 2007. **28**(6): p. 1153-62.
14. Gordon, K.J., et al., *Bone morphogenetic proteins induce pancreatic cancer cell invasiveness through a Smad1-dependent mechanism that involves matrix metalloproteinase-2.* Carcinogenesis, 2009. **30**(2): p. 238-48.
15. Deng, H., et al., *Bone morphogenetic protein-4 is overexpressed in colonic adenocarcinomas and promotes migration and invasion of HCT116 cells.* Exp Cell Res, 2007. **313**(5): p. 1033-44.

16. Cao, Y., et al., *BMP4 inhibits breast cancer metastasis by blocking myeloid-derived suppressor cell activity.* Cancer Res, 2014. **74**(18): p. 5091-102.
17. Gold, M.O. and A.P. Rice, *Targeting of CDK8 to a promoter-proximal RNA element demonstrates catalysis-dependent activation of gene expression.* Nucleic Acids Res, 1998. **26**(16): p. 3784-8.
18. Xu, W., et al., *Mutated K-ras activates CDK8 to stimulate the epithelial-to-mesenchymal transition in pancreatic cancer in part via the Wnt/beta-catenin signaling pathway.* Cancer Lett, 2015. **356**(2 Pt B): p. 613-27.
19. Firestein, R., et al., *CDK8 is a colorectal cancer oncogene that regulates beta-catenin activity.* Nature, 2008. **455**(7212): p. 547-51.
20. Kapoor, A., et al., *The histone variant macroH2A suppresses melanoma progression through regulation of CDK8.* Nature, 2010. **468**(7327): p. 1105-9.
21. Li, X.Y., et al., *siRNA-mediated silencing of CDK8 inhibits proliferation and growth in breast cancer cells.* Int J Clin Exp Pathol, 2014. **7**(1): p. 92-100.
22. Li, X.Y., et al., *MiRNA-107 inhibits proliferation and migration by targeting CDK8 in breast cancer.* Int J Clin Exp Med, 2014. **7**(1): p. 32-40.
23. Alarcon, C., et al., *Nuclear CDKs drive Smad transcriptional activation and turnover in BMP and TGF-beta pathways.* Cell, 2009. **139**(4): p. 757-69.
24. Aragon, E., et al., *A Smad action turnover switch operated by WW domain readers of a phosphoserine code.* Genes Dev, 2011. **25**(12): p. 1275-88.
25. Lamar, J.M., et al., *The Hippo pathway target, YAP, promotes metastasis through its TEAD-interaction domain.* Proc Natl Acad Sci U S A, 2012. **109**(37): p. E2441-50.
26. Zhao, H., et al., *E2A suppresses invasion and migration by targeting YAP in colorectal cancer cells.* J Transl Med, 2013. **11**: p. 317.
27. Hao, Y., et al., *Tumor suppressor LATS1 is a negative regulator of oncogene YAP.* J Biol Chem, 2008. **283**(9): p. 5496-509.
28. Levental, K.R., et al., *Matrix crosslinking forces tumor progression by enhancing integrin signaling.* Cell, 2009. **139**(5): p. 891-906.
29. Seewaldt, V., *ECM stiffness paves the way for tumor cells.* Nat Med, 2014. **20**(4): p. 332-3.
30. Lessey, E.C., C. Guilluy, and K. Burridge, *From mechanical force to RhoA activation.* Biochemistry, 2012. **51**(38): p. 7420-32.
31. Jaalouk, D.E. and J. Lammerding, *Mechanotransduction gone awry.* Nat Rev Mol Cell Biol, 2009. **10**(1): p. 63-73.
32. Osborne, L.D., et al., *TGF-beta regulates LARG and GEF-H1 during EMT to impact stiffening response to force and cell invasion.* Mol Biol Cell, 2014.
33. Dupont, S., et al., *Role of YAP/TAZ in mechanotransduction.* Nature, 2011. **474**(7350): p. 179-83.
34. Leight, J.L., et al., *Matrix rigidity regulates a switch between TGF-beta1-induced apoptosis and epithelial-mesenchymal transition.* Mol Biol Cell, 2012. **23**(5): p. 781-91.

35. Tilghman, R.W., et al., *Matrix rigidity regulates cancer cell growth and cellular phenotype.* PLoS One, 2010. **5**(9): p. e12905.
36. Yu, P.B., et al., *Dorsomorphin inhibits BMP signals required for embryogenesis and iron metabolism.* Nat Chem Biol, 2008. **4**(1): p. 33-41.
37. Piccolo, S., S. Dupont, and M. Cordenonsi, *The Biology of YAP/TAZ: Hippo Signaling and Beyond.* Physiol Rev, 2014. **94**(4): p. 1287-1312.
38. Porter, D.C., et al., *Cyclin-dependent kinase 8 mediates chemotherapy-induced tumor-promoting paracrine activities.* Proc Natl Acad Sci U S A, 2012. **109**(34): p. 13799-804.
39. Hoadley, K.A., et al., *Multiplatform analysis of 12 cancer types reveals molecular classification within and across tissues of origin.* Cell, 2014. **158**(4): p. 929-44.
40. Ampuja, M., et al., *The impact of bone morphogenetic protein 4 (BMP4) on breast cancer metastasis in a mouse xenograft model.* Cancer Lett, 2016.
41. Fang, W.T., et al., *Downregulation of a putative tumor suppressor BMP4 by SOX2 promotes growth of lung squamous cell carcinoma.* Int J Cancer, 2014. **135**(4): p. 809-19.
42. Fryer, C.J., J.B. White, and K.A. Jones, *Mastermind recruits CycC:CDK8 to phosphorylate the Notch ICD and coordinate activation with turnover.* Mol Cell, 2004. **16**(4): p. 509-20.

**Appendix A**
**OvCa429 Data**

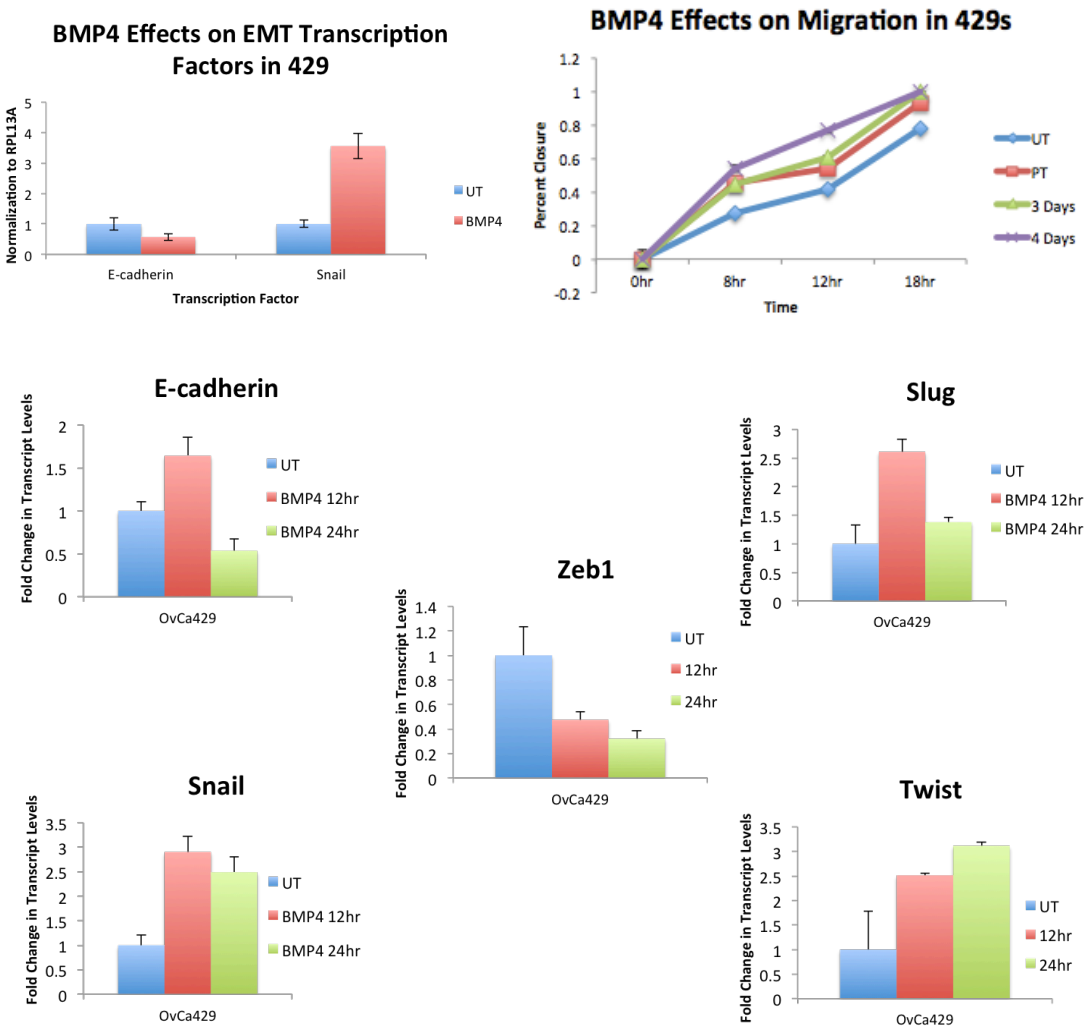


Figure A.1: Effect of BMP on Transcript Levels & Migration (A) Effect of BMP4 on EMT Transcript Levels. Expt 2-11. (B) Effect of BMP4 on EMT Transcript Levels Time Course. Expt 2-34. (C) Effect of BMP4 on migration. Expt 2-17.

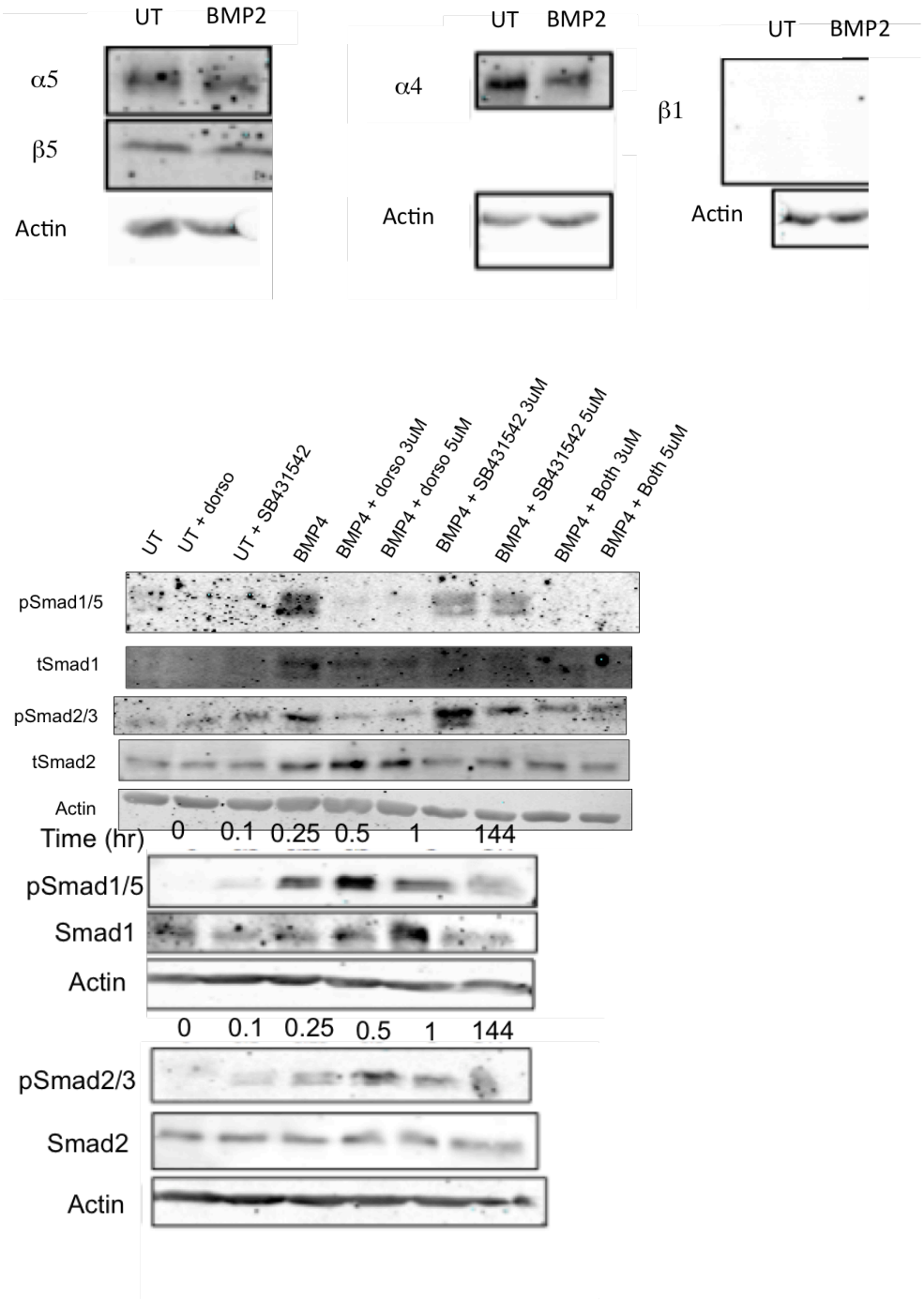


Figure A.2: Effects of BMP on Smad Signaling (A) Effect of BMP2 on Integrin Levels. Expt 2-1. (B) Role of Alk3/6 & Alk5/7 on BMP4 Induced EMT. Expt 2-41. (C) Effect of BMP4 on Smad Signaling. Expt 2-14.

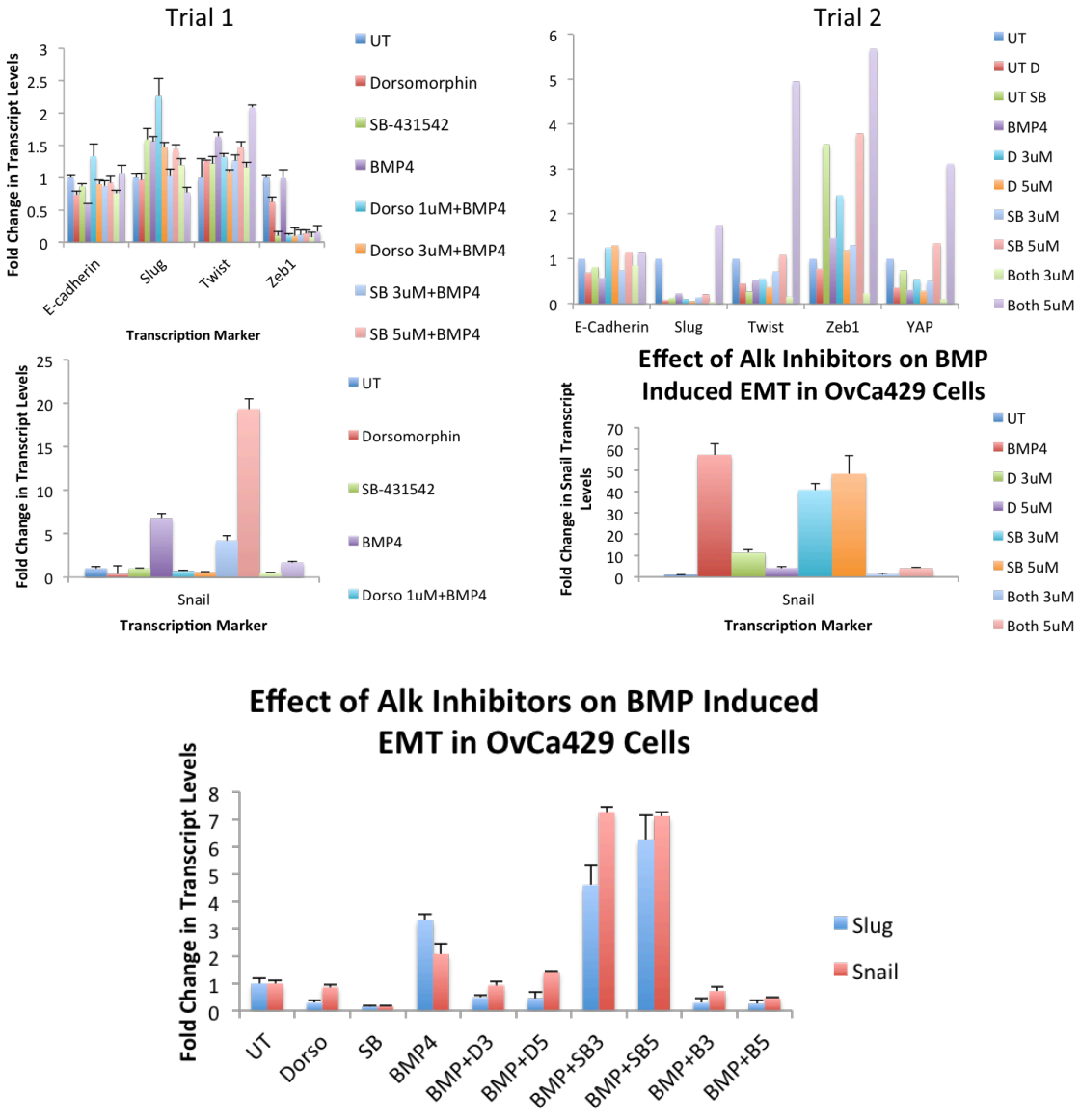





Figure A.3: Role of Alk3/6 & Alk5/7 on BMP4 Induced EMT Transcript Levels. Expt 2-39.

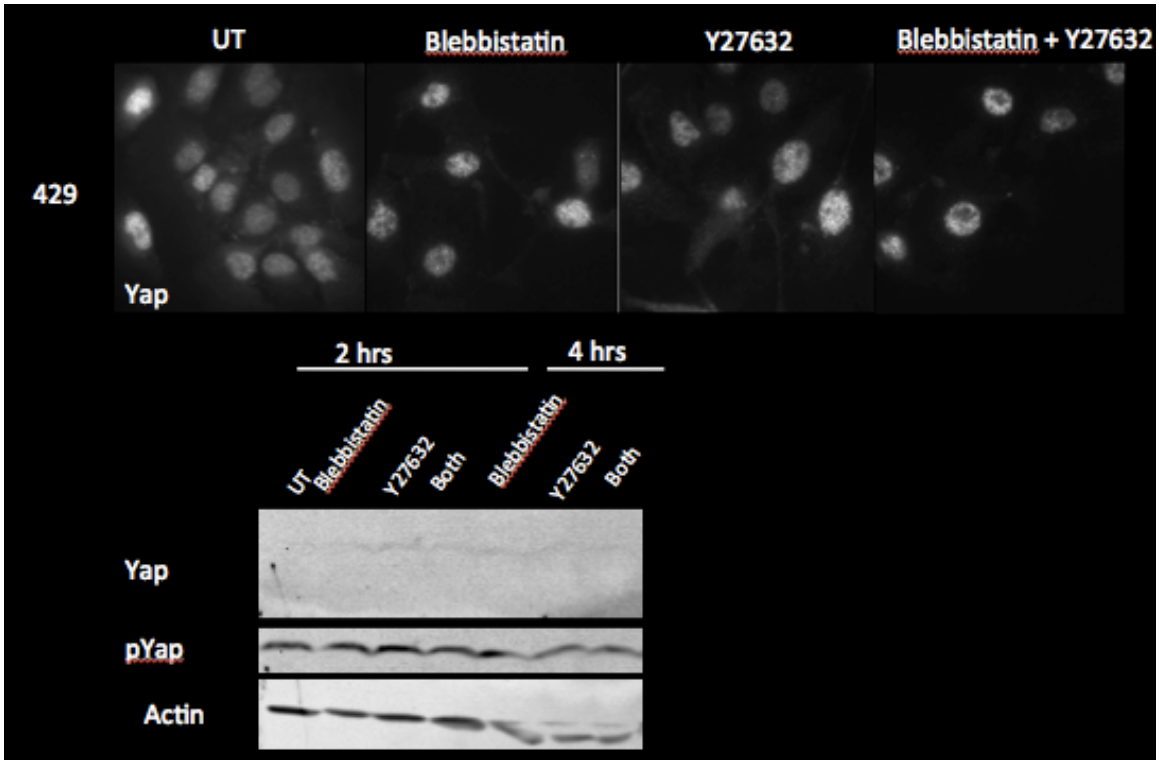


Figure A.4: Effects of Blebbistatin and Y27632 on Yap Localization. Expt. 2-28.

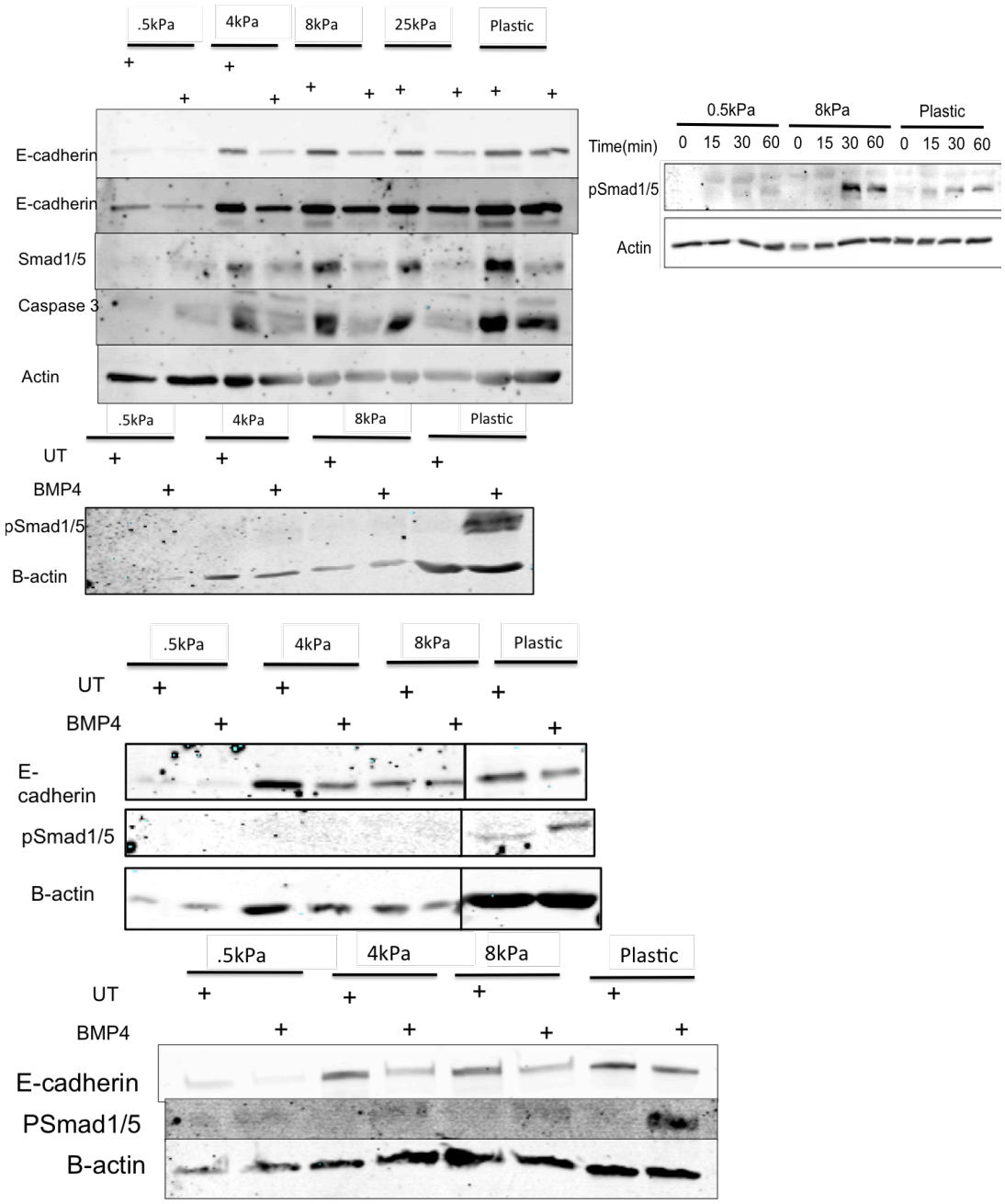


Figure A.5: Effects of Matrix Rigidity on BMP4 Induced EMT 1. (A) Expt. 2-24. (B-C) Expt 2-13. (D) Expt 2-16.

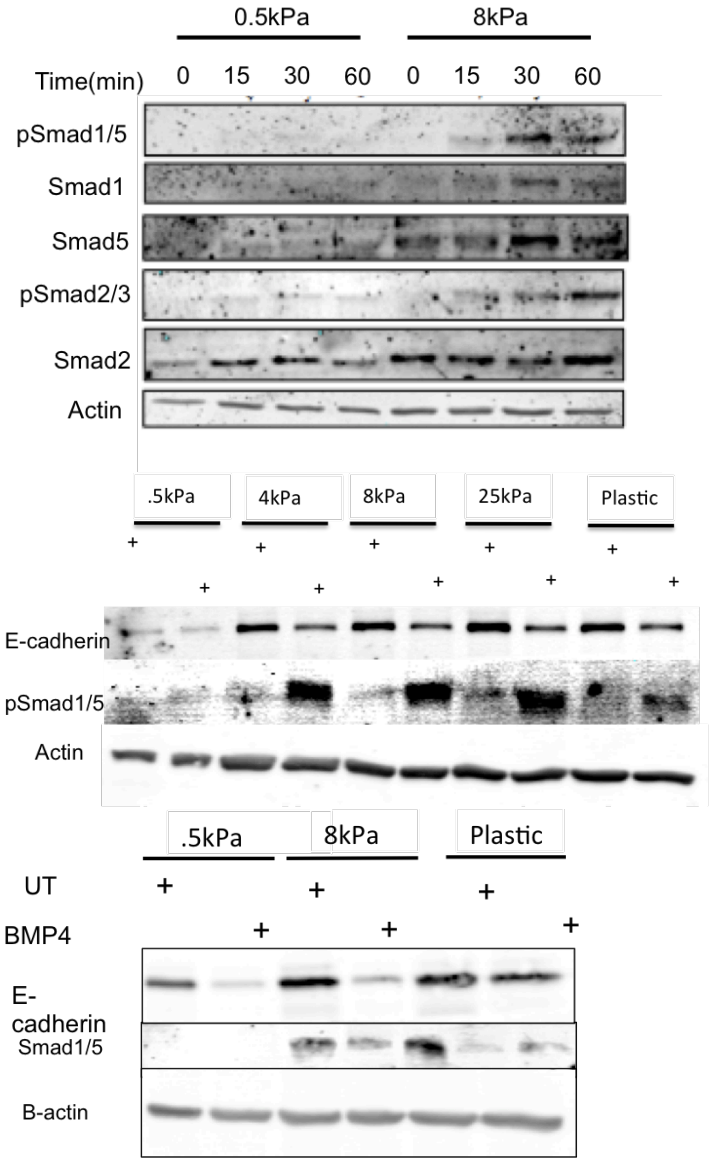


Figure A.6: Effects of Matrix Rigidity on BMP4 Induced EMT 2. (A) Expt.3-8 (B) Expt 2-24. (C) Expt. 2-27

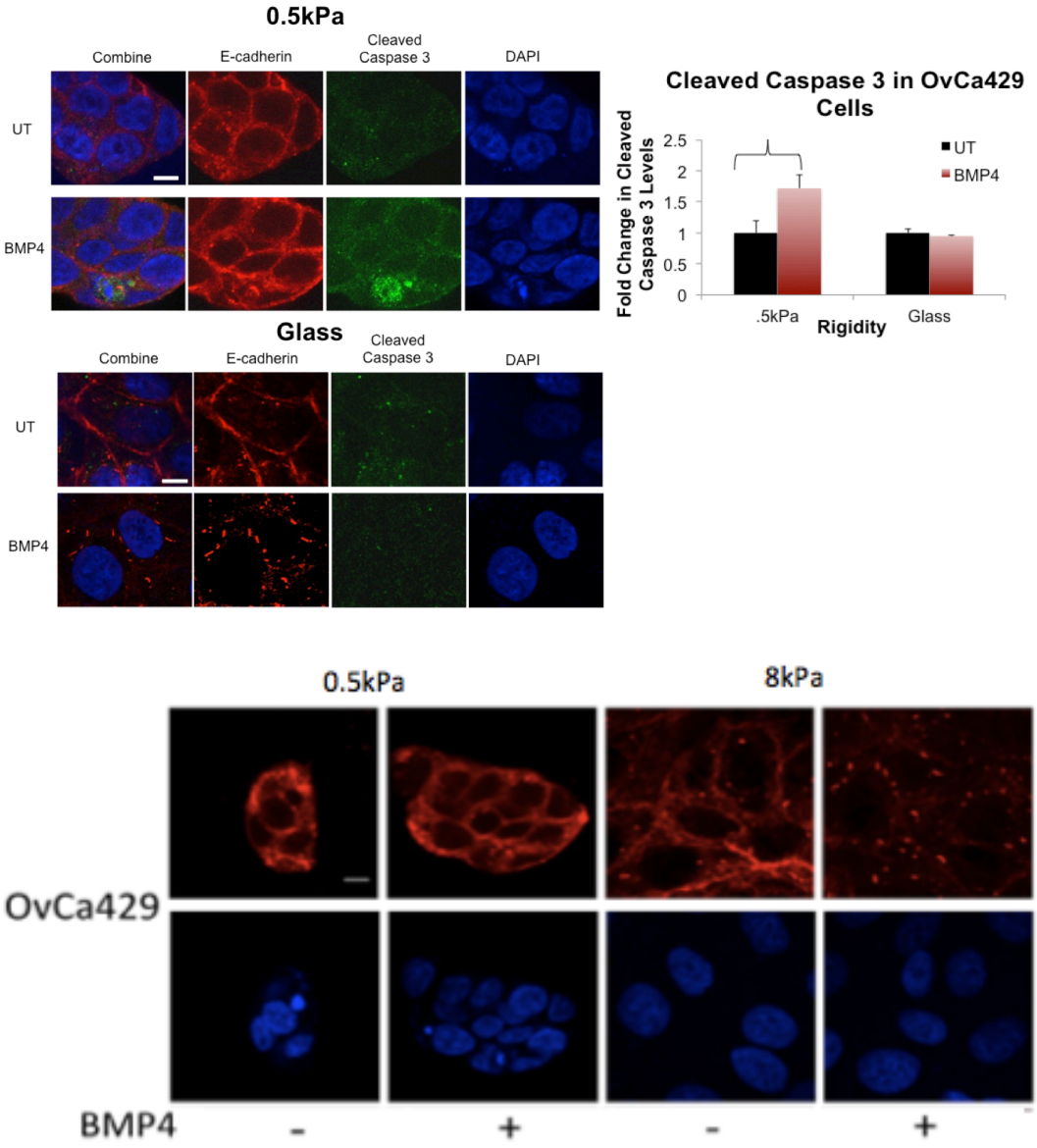


Figure A.7: Effects of Matrix Rigidity on BMP4 Induced EMT and Apoptosis. (A-B) Expt. 2-22

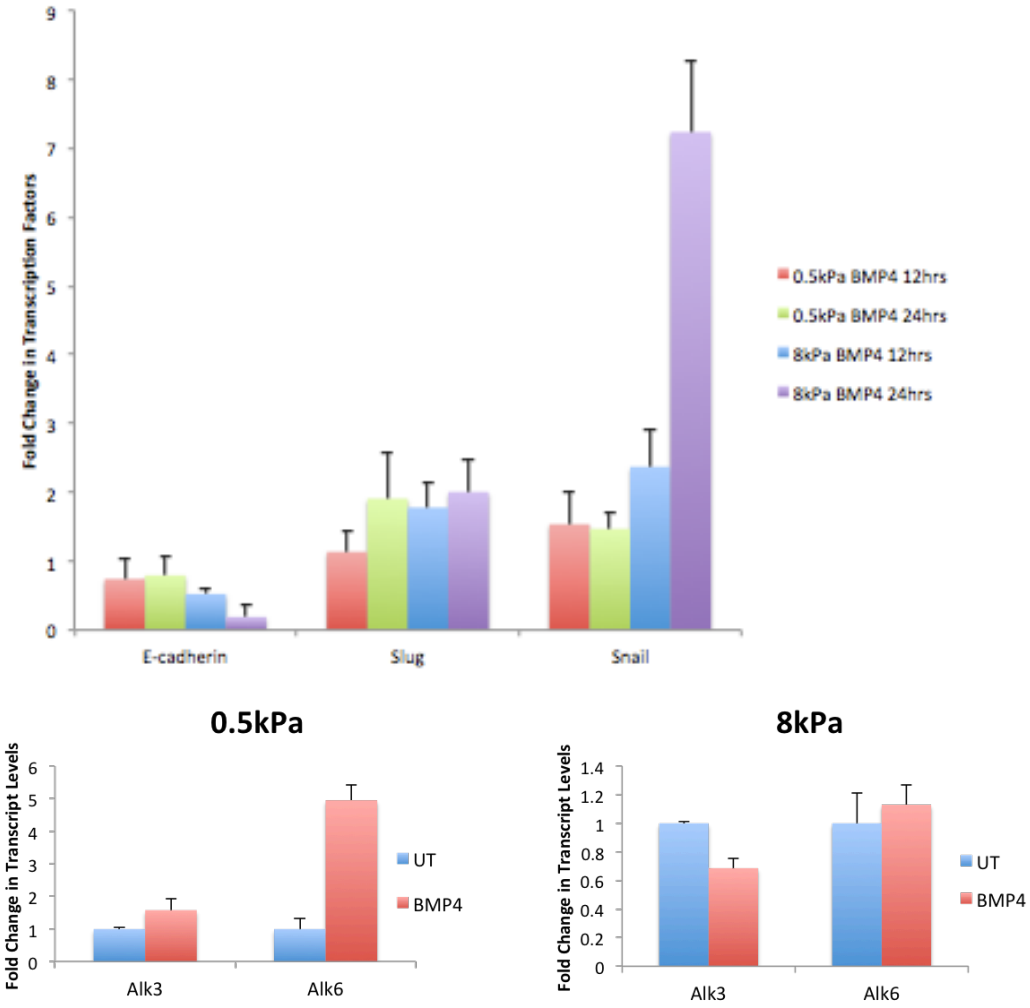


Figure A.8: Effect of Matrix Rigidity on BMP Induced EMT/Receptor Levels (A) Effects of Matrix Rigidity on EMT Transcript Levels (Time Course) Expt 3-15(B) Effects of Matrix Rigidity on Alk3/6 Receptor Levels. Expt 3.12

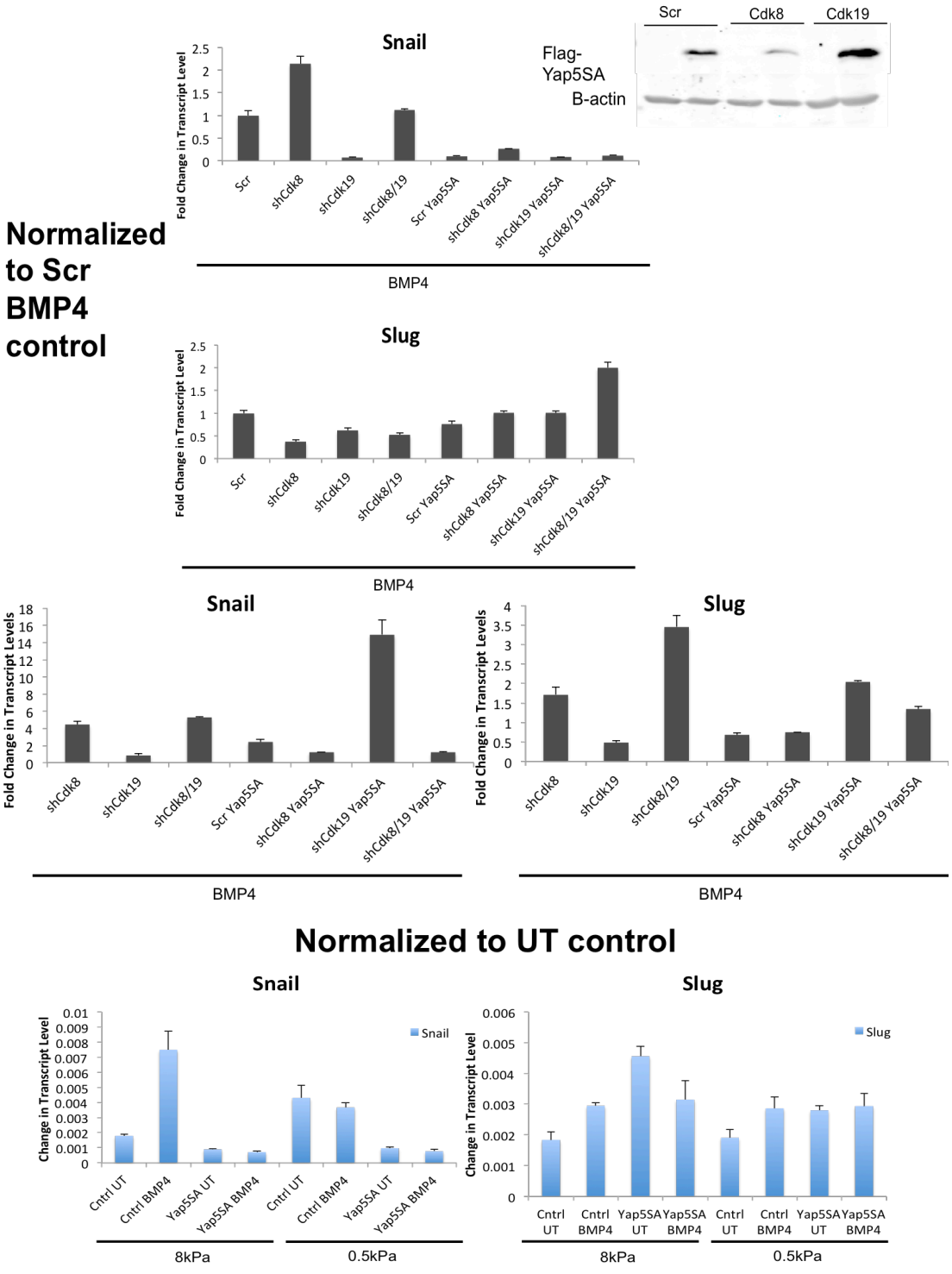


Figure A.9: Effect of Yap5SA on BMP Induced EMT (A-B) Effect of Yap5SA on BMP4 EMT. Expt 4-8. (C) Effect of Matrix Rigidity and Yap 5SA on BMP4 EMT. Expt 4-19

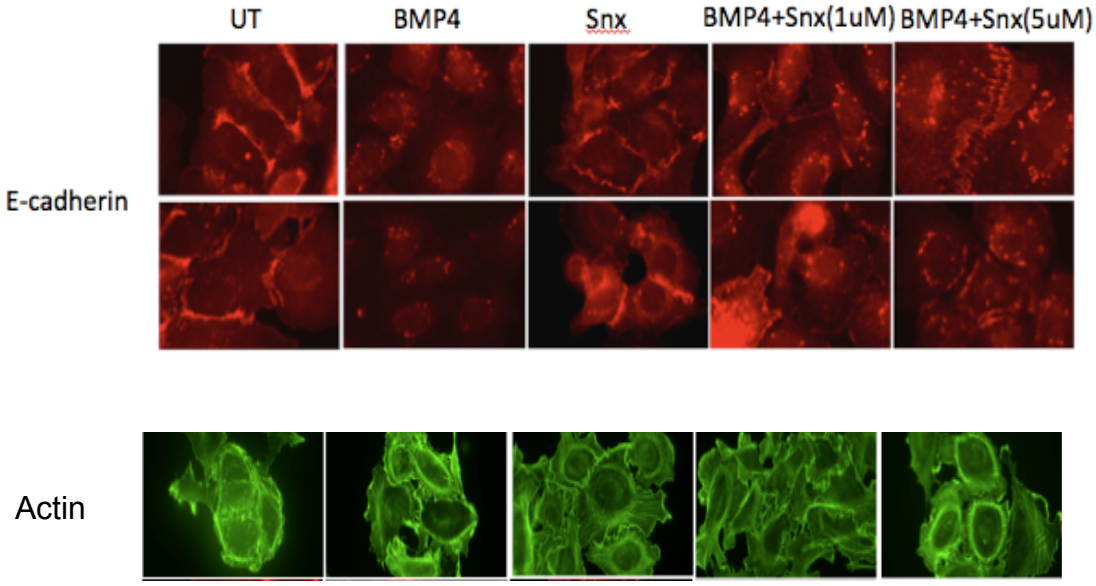


Figure A.10: Effects of SnxB on BMP4 Induced EMT (A) E-cadherin (B) Actin (A-B) Expt 3-19

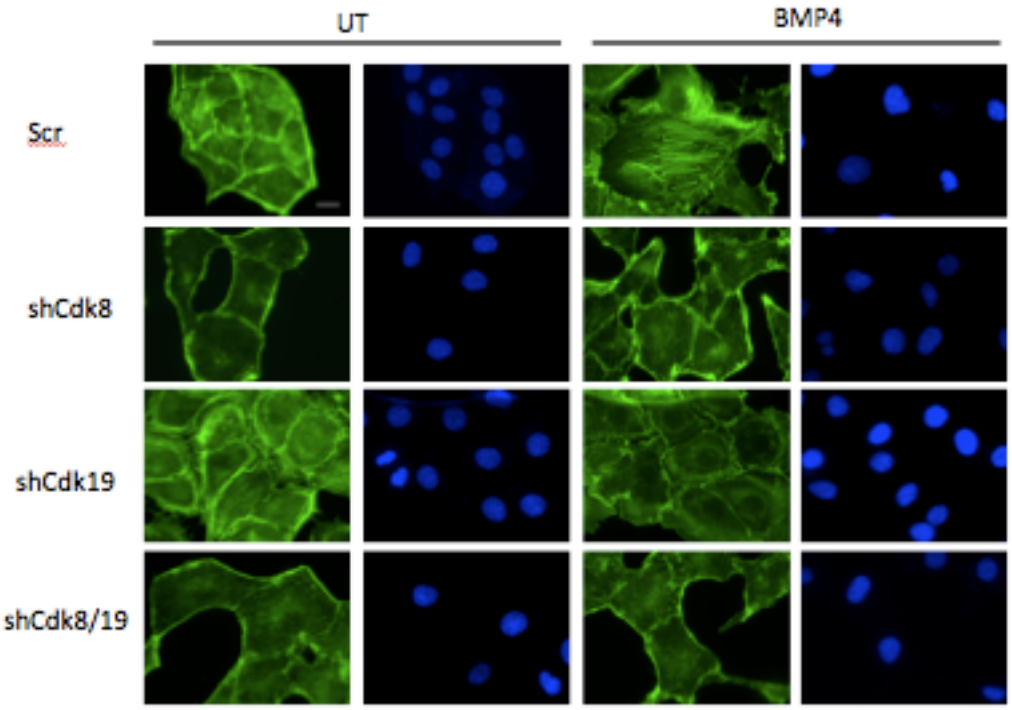


Figure A.11: Effects of shCdk8 and shCdk19 on BMP4 Induced EMT. Expt. 4-5.

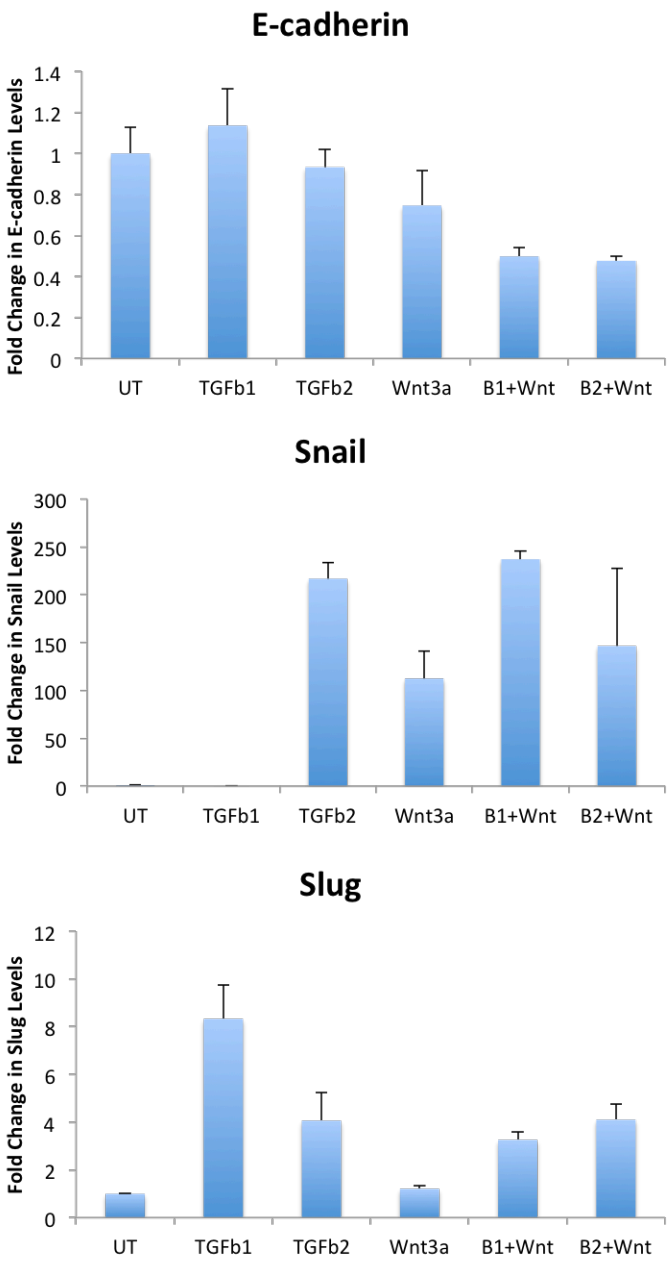


Figure A.12: Effect of Wnt3a and Tgf-β1/2 on EMT. Expt 2-42.

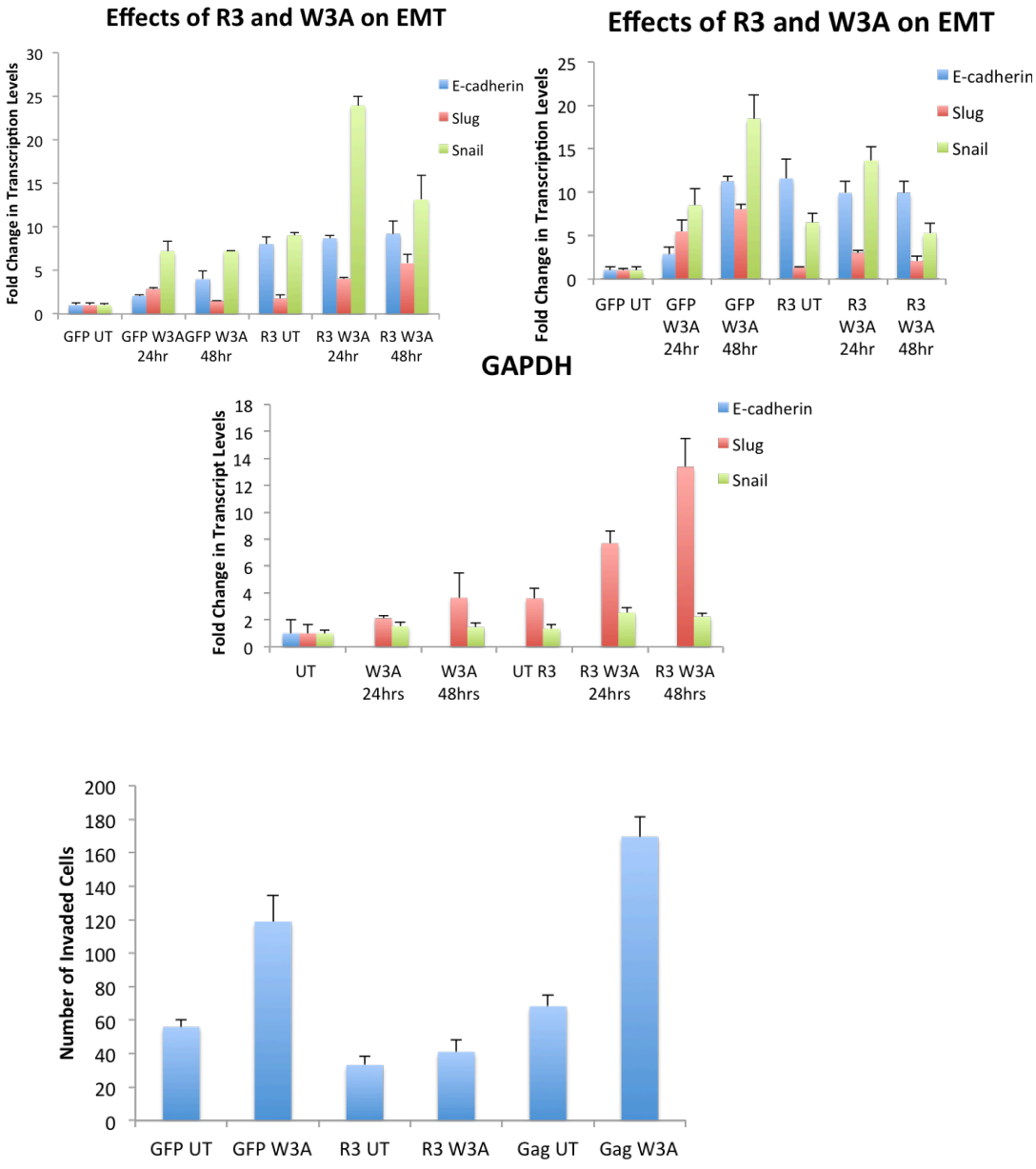


Figure A.13: Effects of R3 and Wnt3a on EMT. (A-C) Transcript Levels. Expt 3-11. (D) Effects of R3 and deltaGAG on Wnt3a Invasion. Expt 3-26.

**Appendix B**
**Panc1 Data**

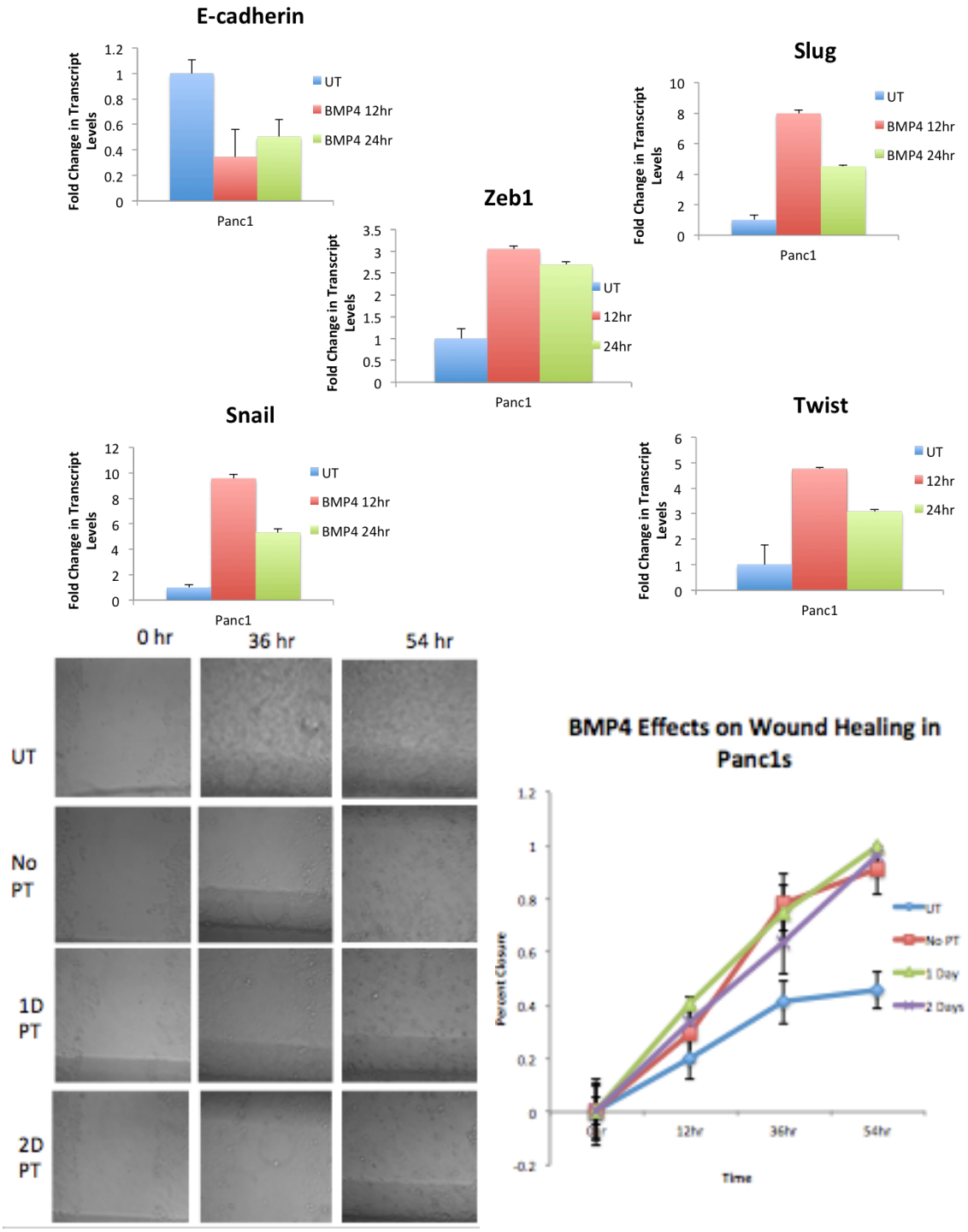


Figure B.1: Effects of BMP on Migration (A) Effects of BMP4 on EMT over time. Expt 2-34. (B-C) Effects of BMP4 on migration. Expt 2-12.

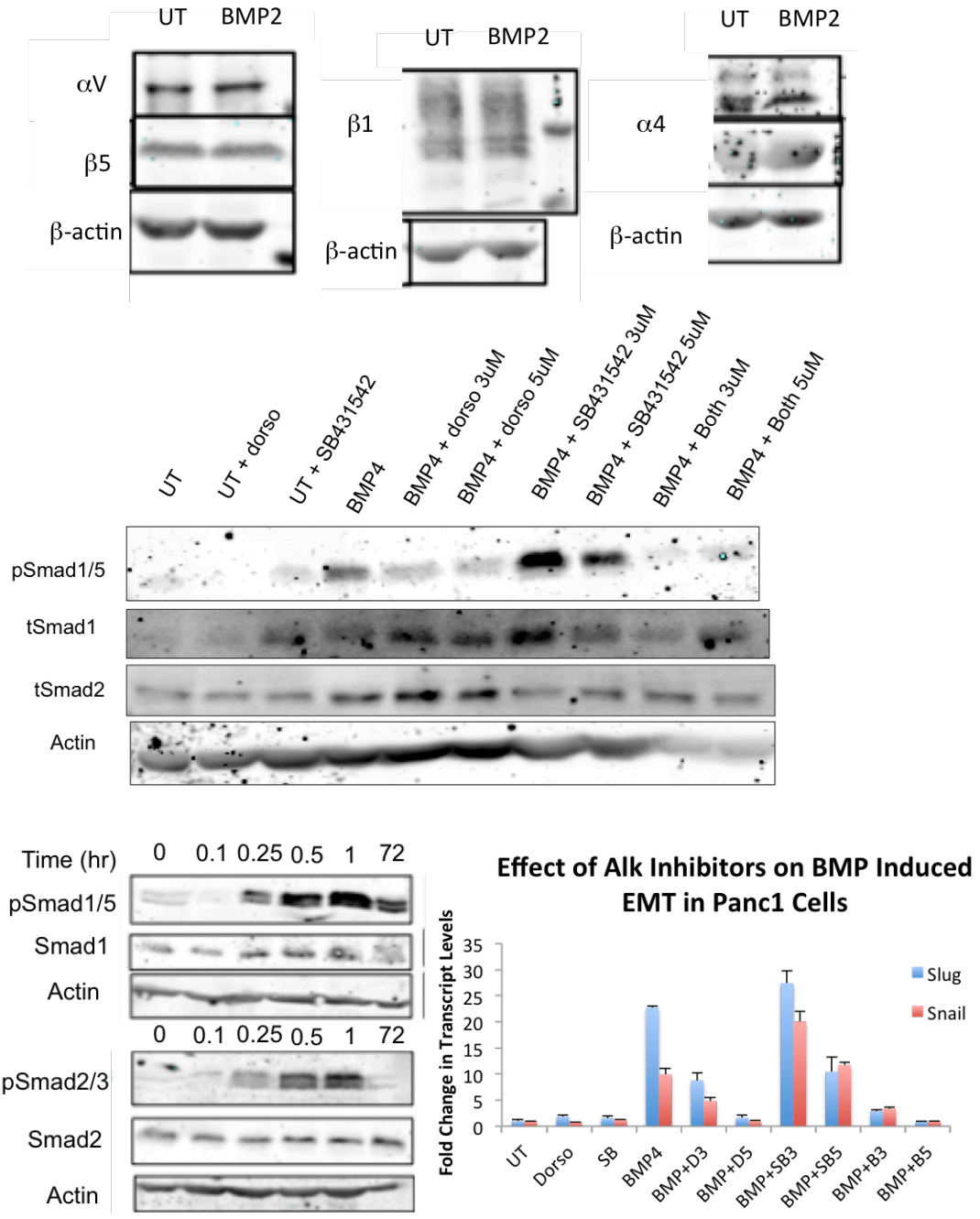


Figure B.2: Role of BMP on Integrins and Smad Signaling (A) Effects of BMP2 on Integrin Levels. Expt 2-1. (B-C) Role of Alk3/6 and Alk5/7 on BMP4 Induced EMT (B) Western analysis. Expt 2-41 (C) qPCR. Expt 2-39. (D) Effect of BMP4 on Smad Signaling. Expt 2-14.

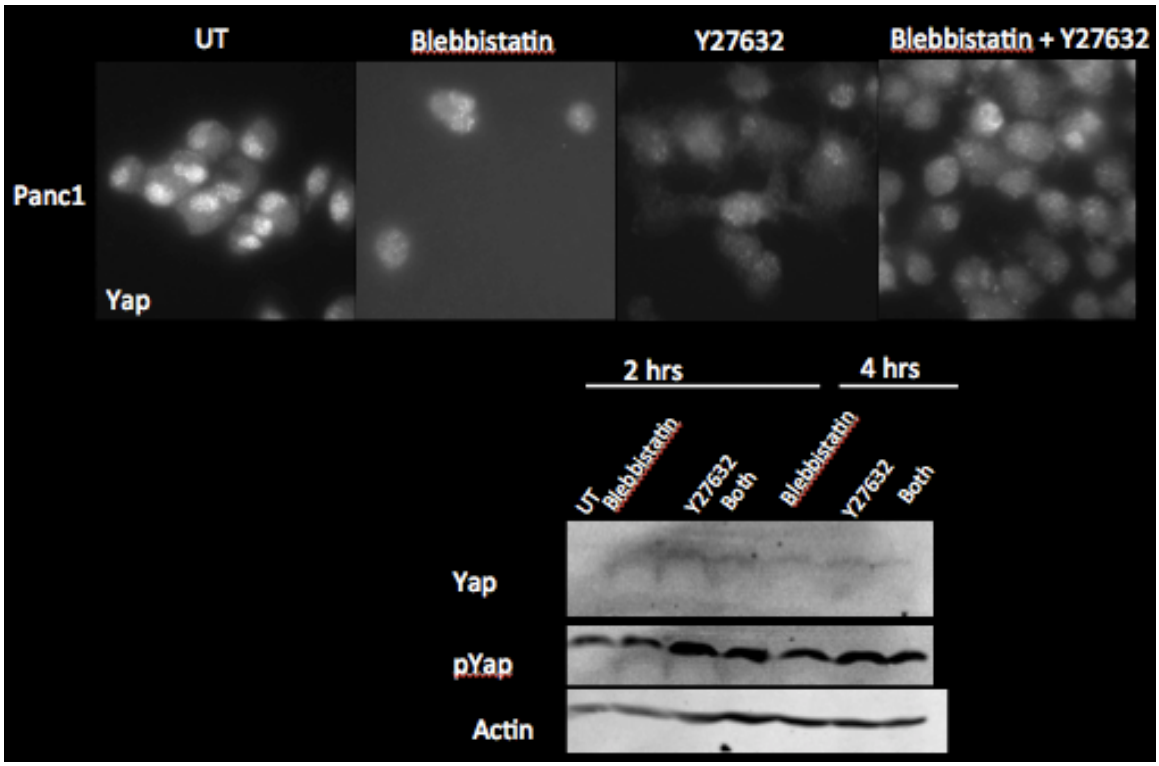


Figure B.3: Effect of Blebbistatin and Y27632 on Yap Localization

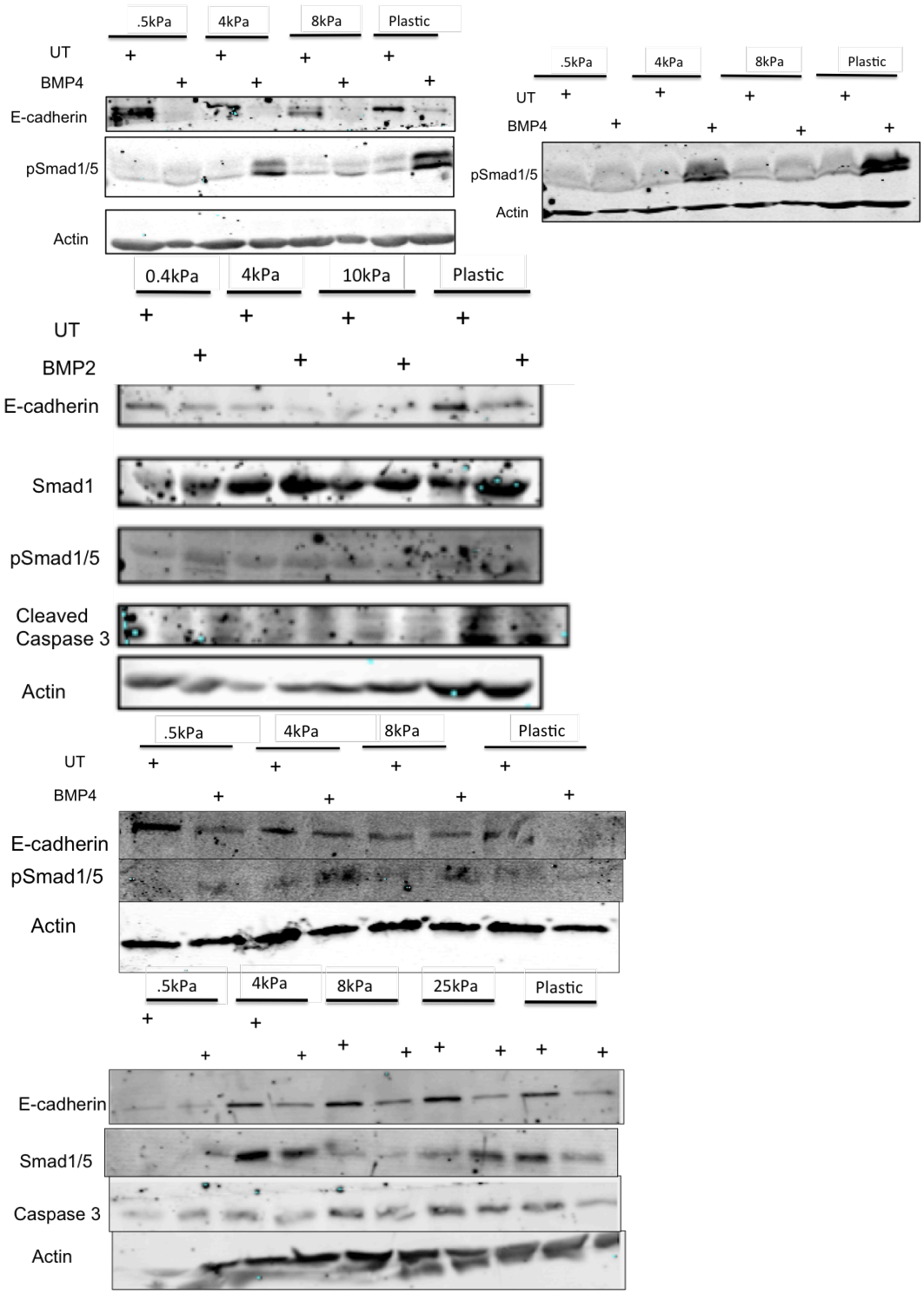


Figure B.4: Effects of Matrix Rigidity on BMP4 Induced EMT 1 (A-B, D-E). (A-B) Expt 2-13. (D) Expt. 2-16. (E) Expt 2-24. (B) Effects of Matrix Rigidity on BMP2 Induced EMT. Expt 2-3.

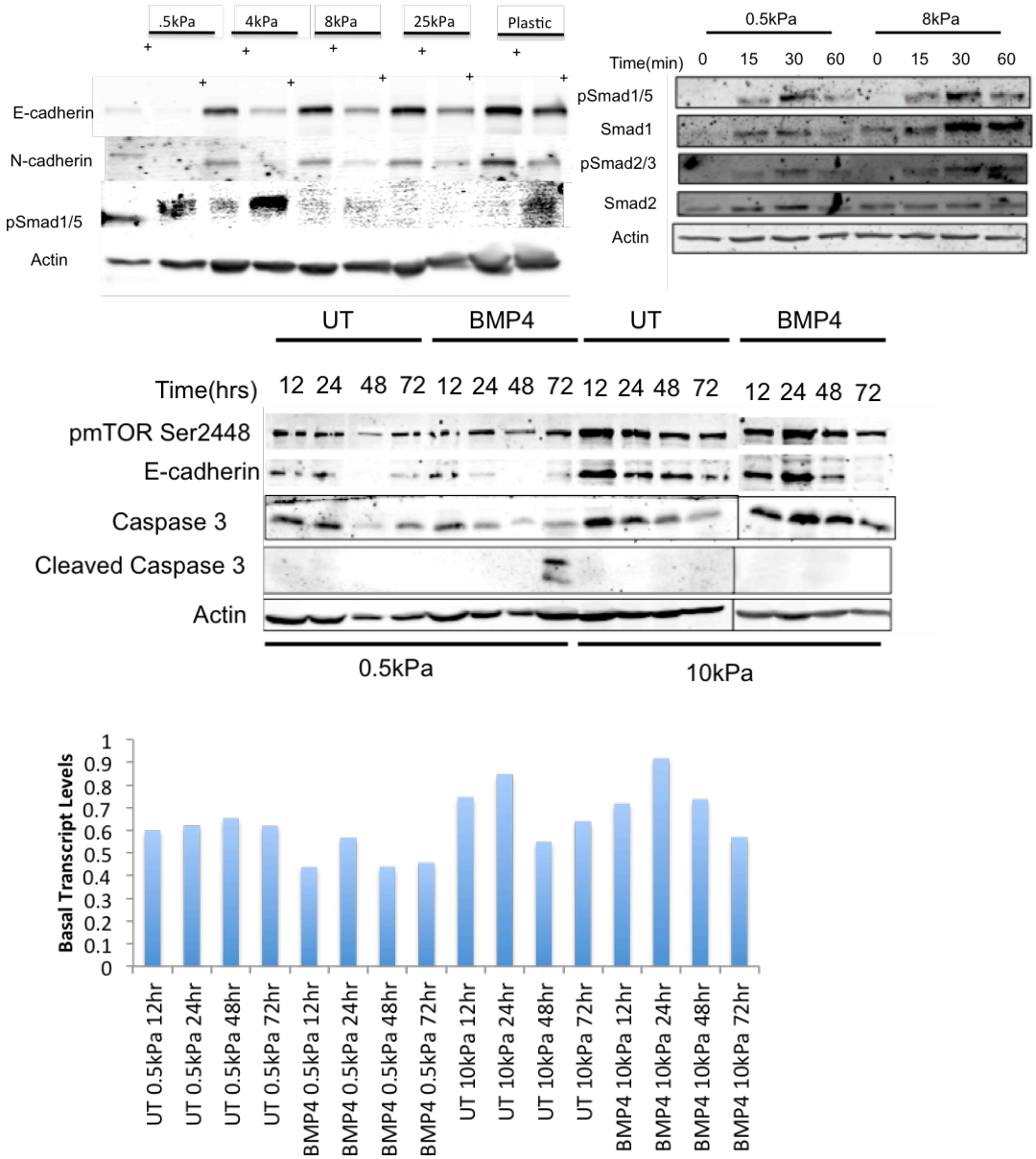





Figure B.5: Effects of Matrix Rigidity on BMP4 Induced EMT 2 (A-C), Apoptosis, and Autophagy (C-D). (A) Expt 2-24. (B) Expt 3-8. (C-D) Expt. 3-9.

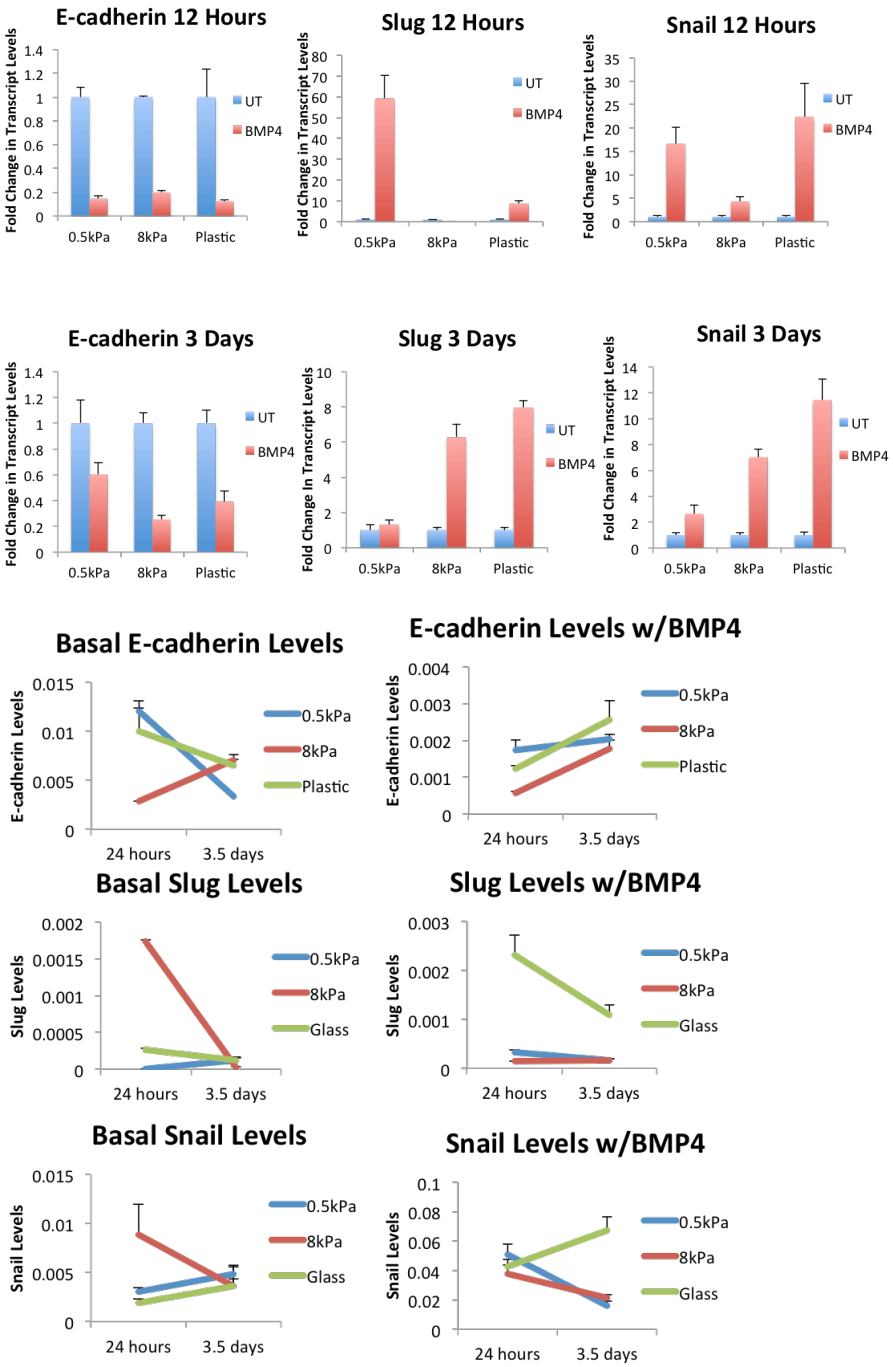


Figure B.6: Effects of Matrix Rigidity on BMP4 induced EMT 3. (A-B) (Time Course). Expt 3-5.

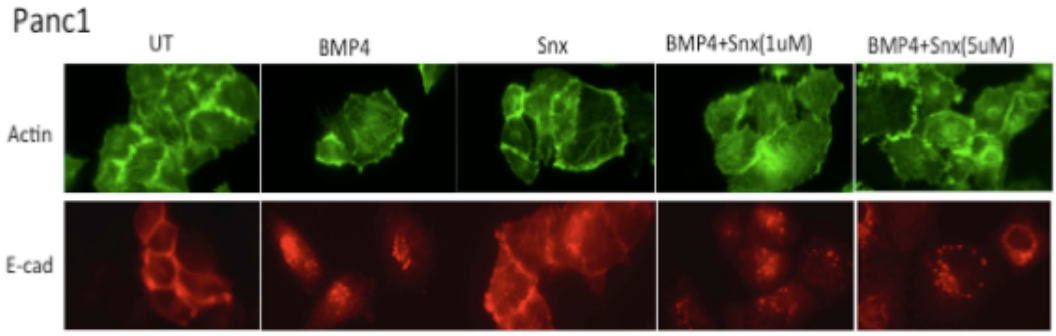


Figure B.7: Effect of SnxB on BMP4 Induced EMT IF. (A) Actin (B) E-cadherin Expt. 3-19

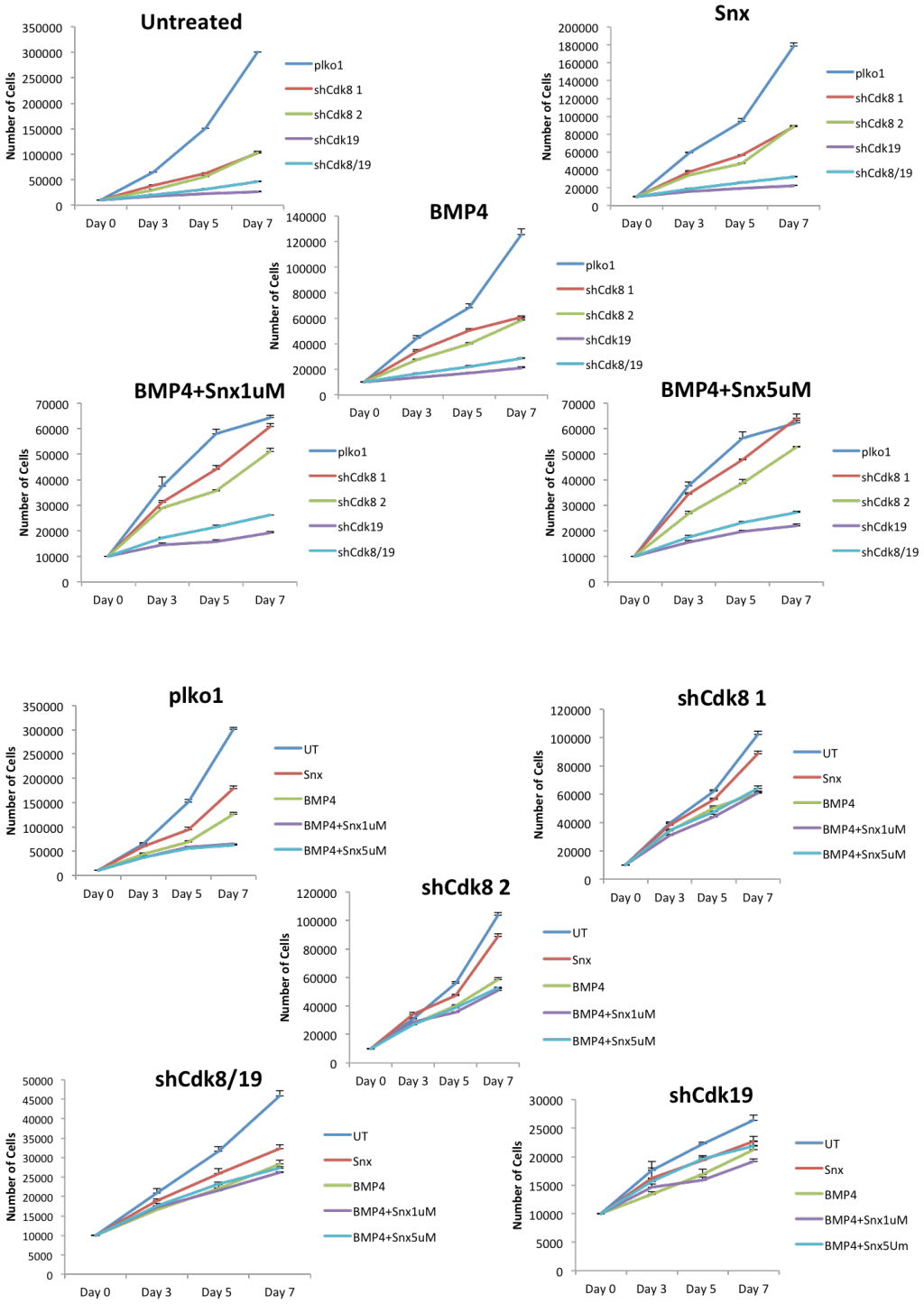


Figure B.8: Effect of BMP4, Snx, shCdk8, and shCdk9 on Cell Proliferation (A) Graphed by Treatment (B) Graphed by Cell Line. Expt 3-25

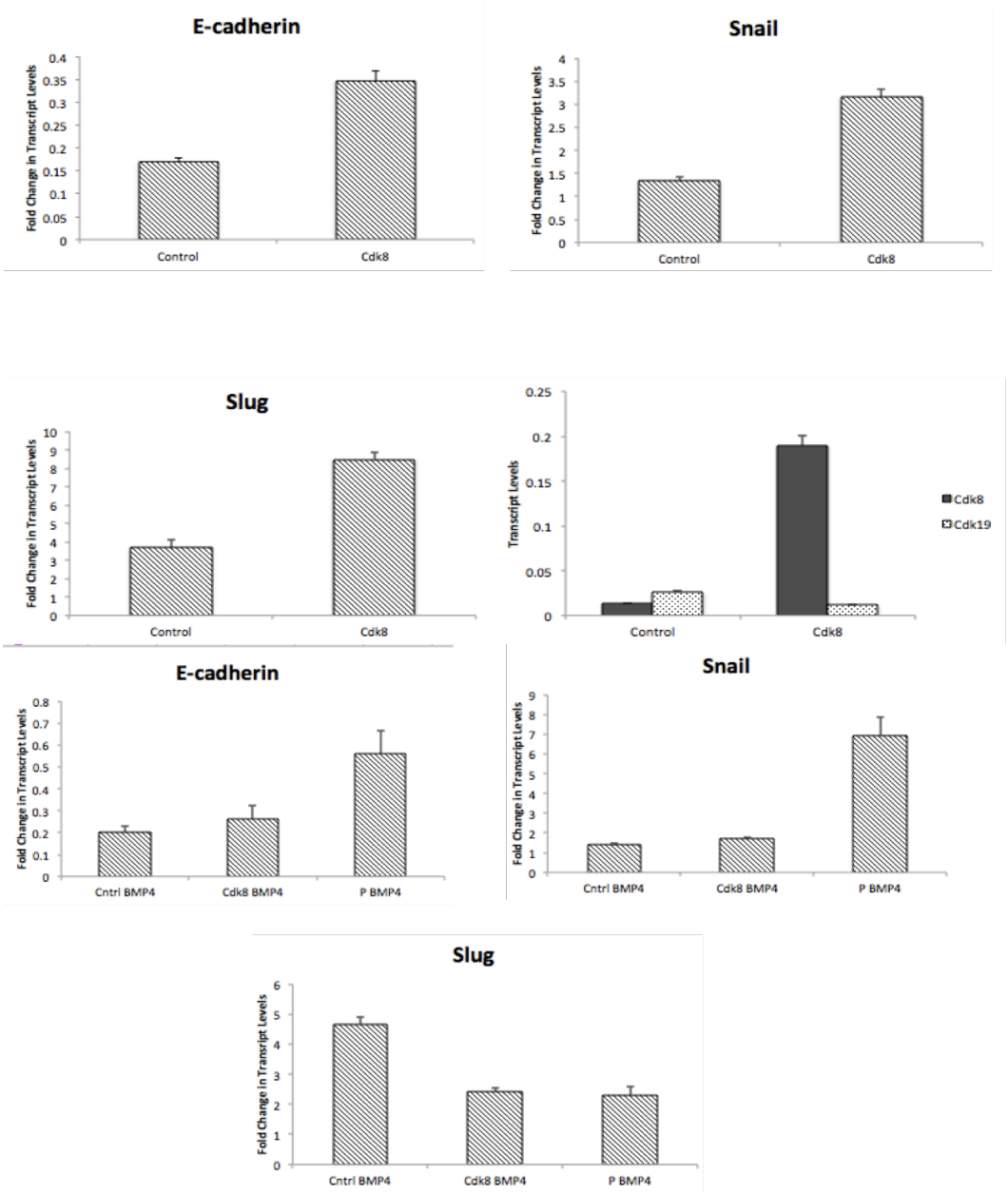


Figure B.9: Effect of shCdk8 (kinase dead) on BMP4 Induced EMT. (A-B) Expt. 3-4.

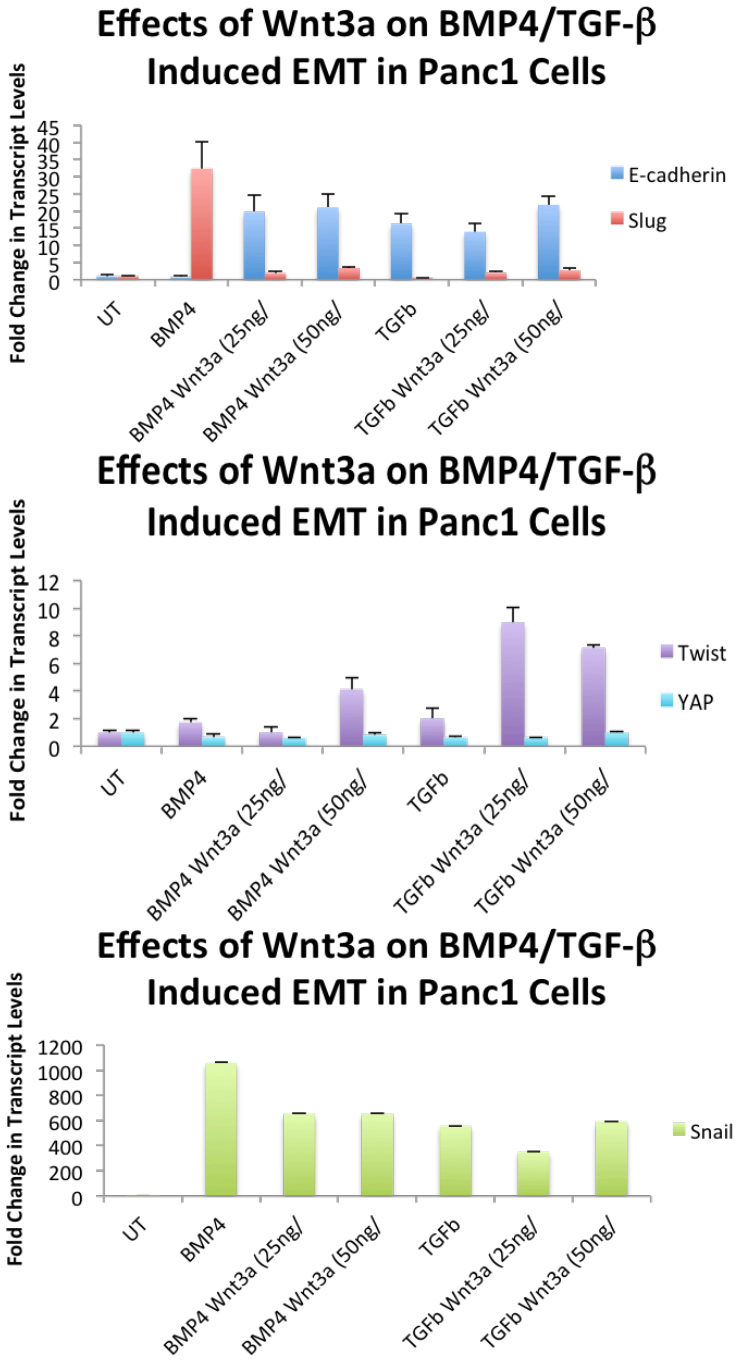


Figure B.10: Effects of Wnt3a on BMP4/Tgfβ-1 Induced EMT. (A-C) Expt 2-42.

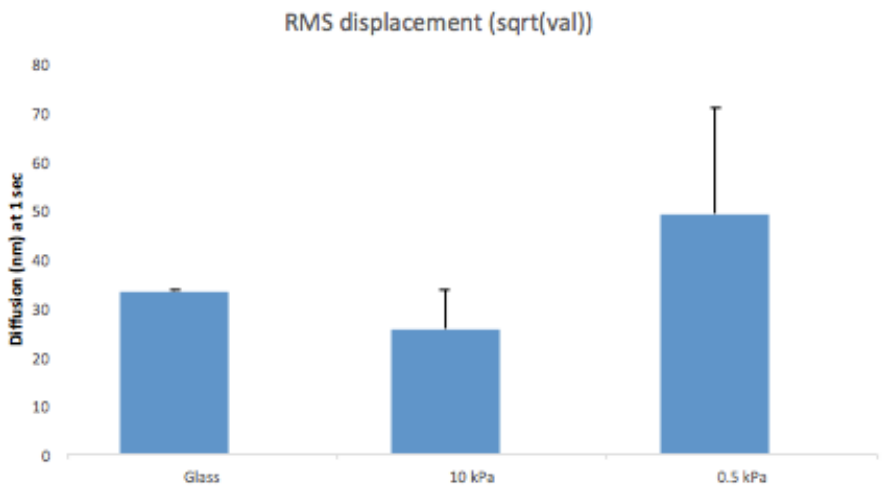


Figure B.11: Effects of Matrix Rigidity on Cell Stiffness. On server.

**Appendix C**
**CT26 Data**

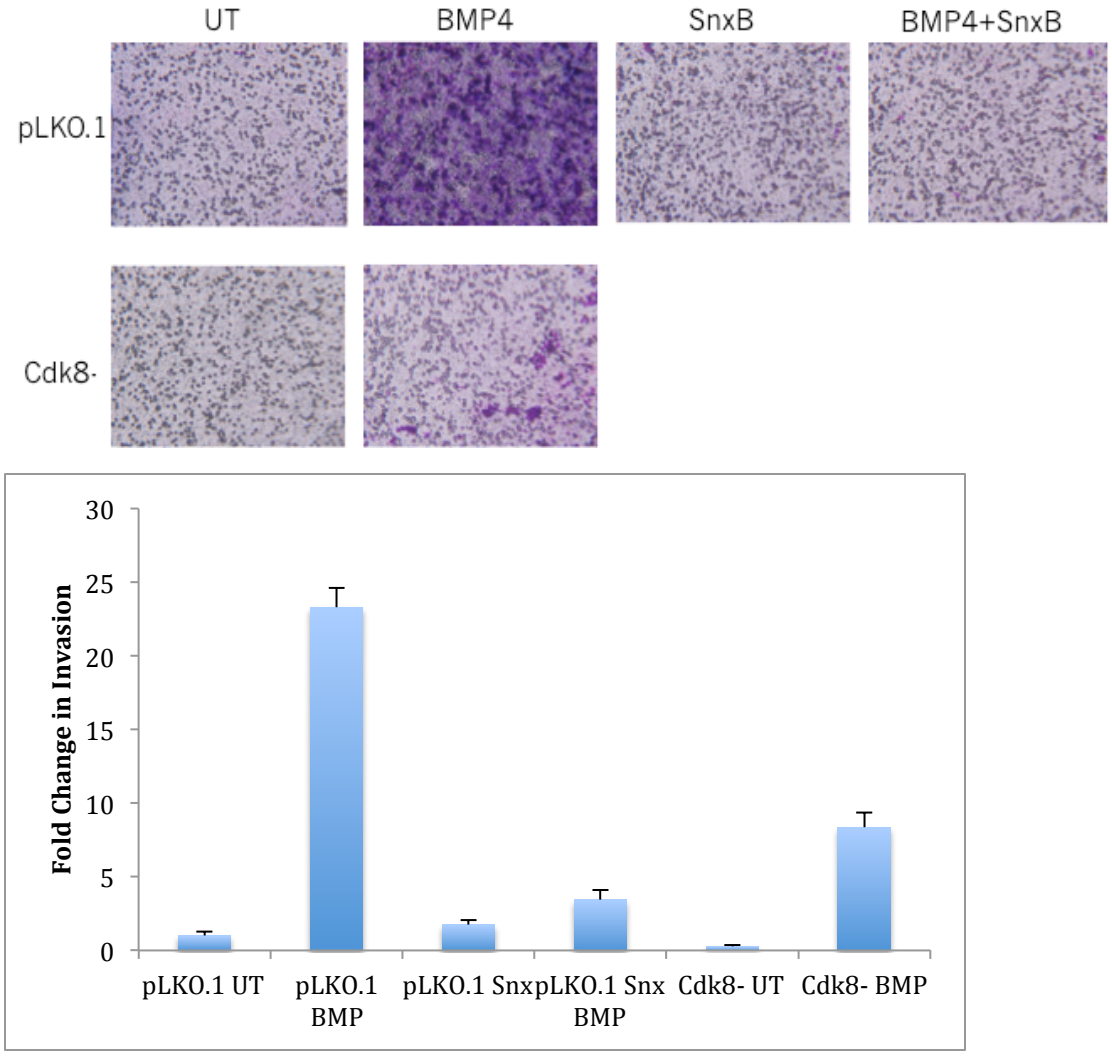


Figure C.1: Effect of SnxB on CT26 Cell Invasion. Expt S-22.

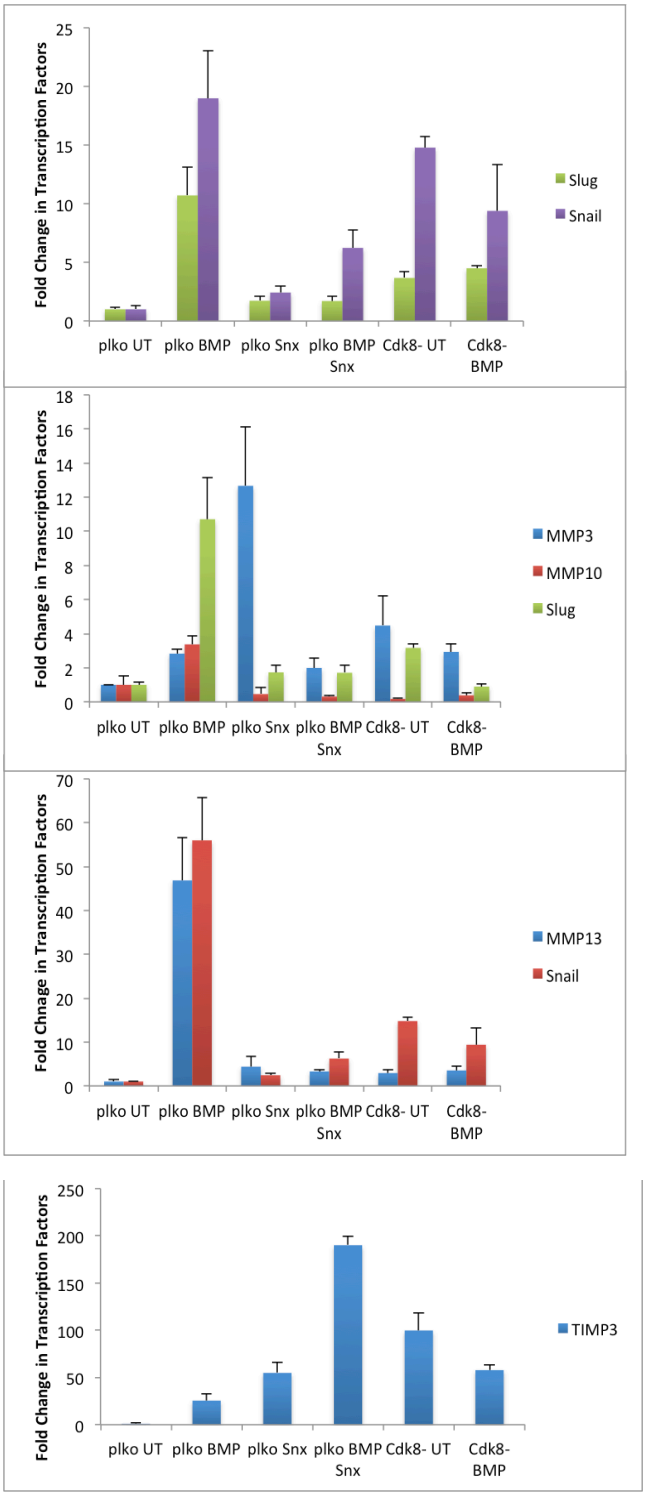


Figure C.2: Effects of SnxB on BMP4 Induced EMT. Expt. S-23.

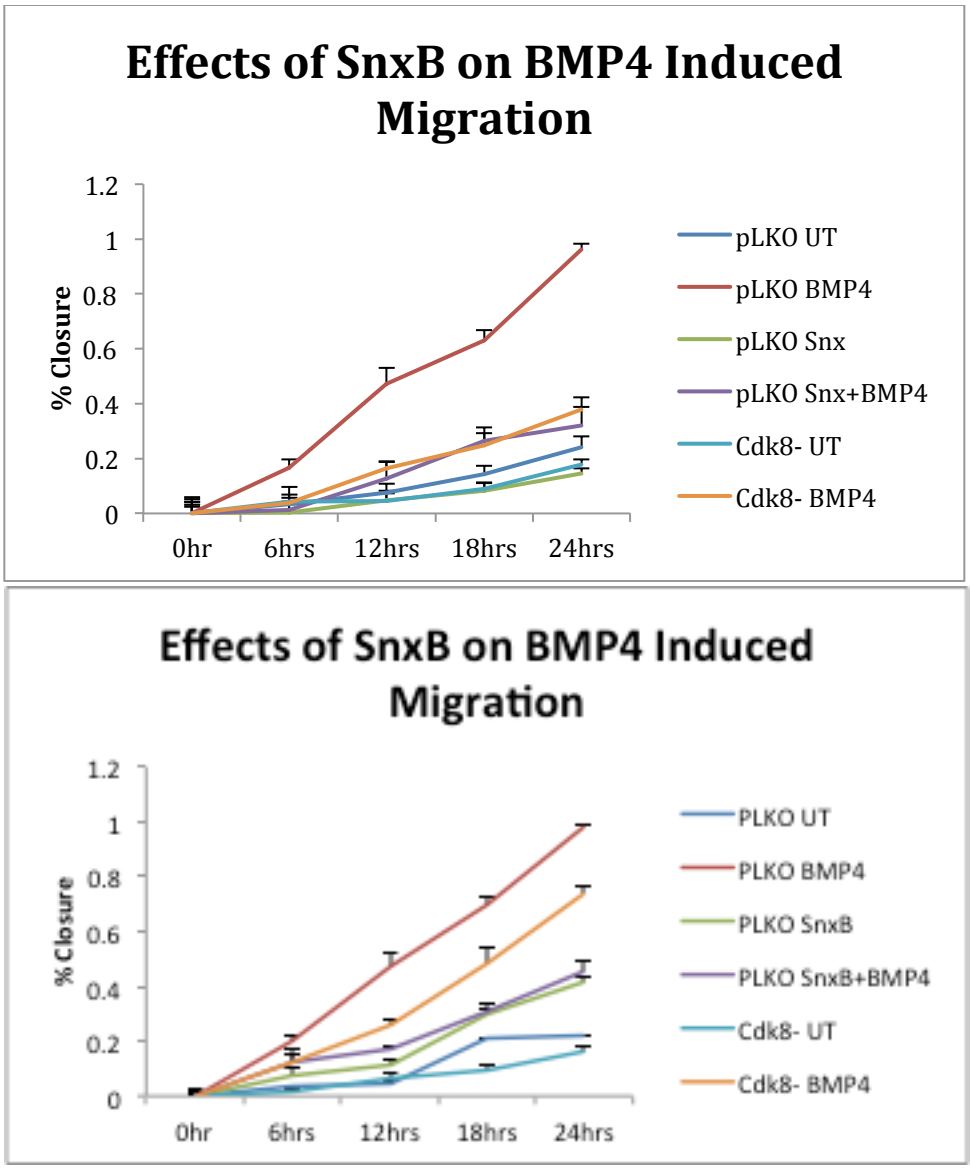


Figure C.3: Effects of SnxB and shCdk8 on CT26 Cell Migration (with repeat). Expt. S-21.

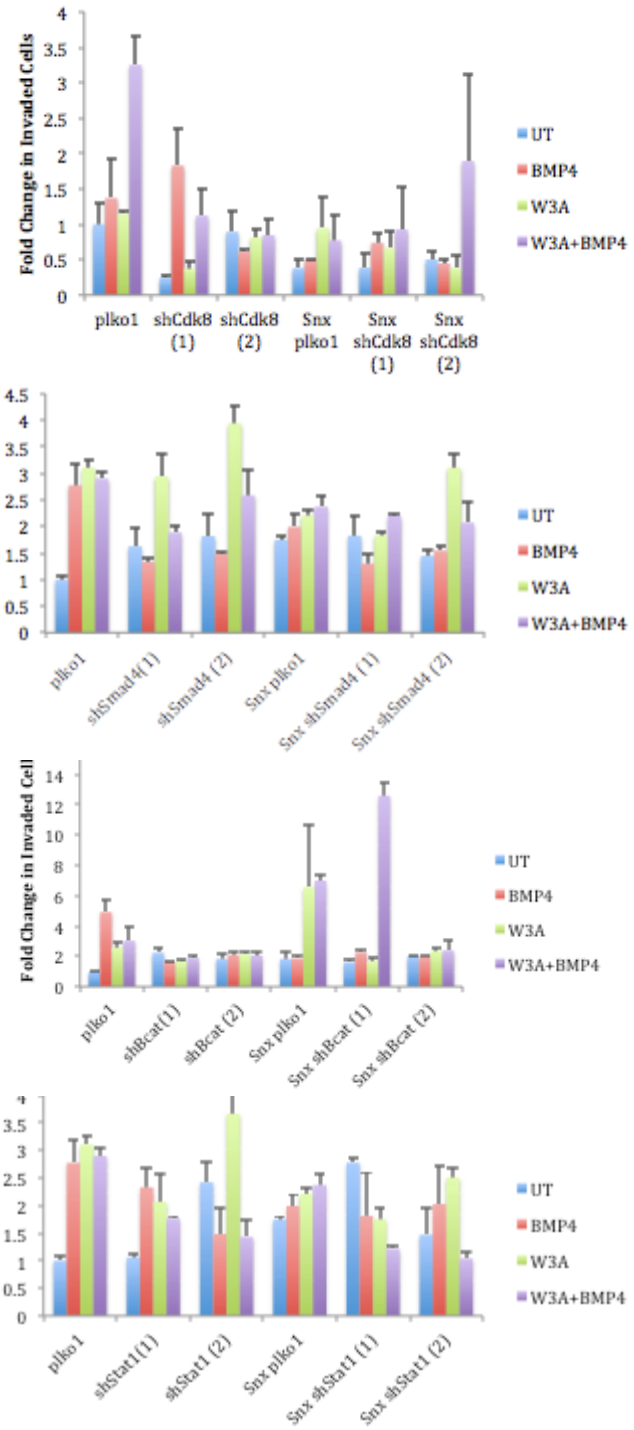


Figure C.4: Effects of SnxB, shCdk8, shSmad4, & shB-catenin on Invasion 1. shCdk8 (A), shSmad4 (B), shBcatenin (C), and shStat1 (D) on BMP4 Induced EMT. Expts. S-27 (A), S-29(B,D), and S-28 (C)

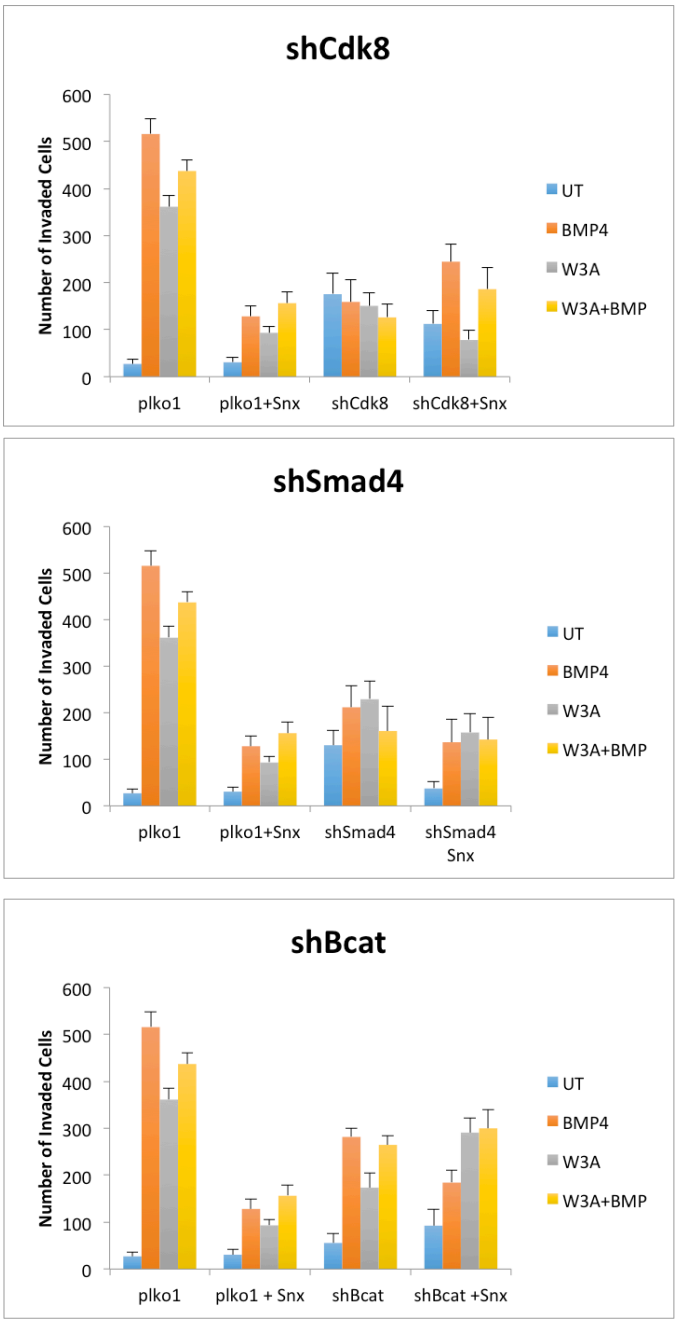


Figure C.5: Effects of SnxB, shCdk8, shSmad4, & shB-catenin on Invasion 2. shCdk8 (A), shSmad4 (B), and shBcatenin (C) on BMP4 Induced EMT. Expt S-31.

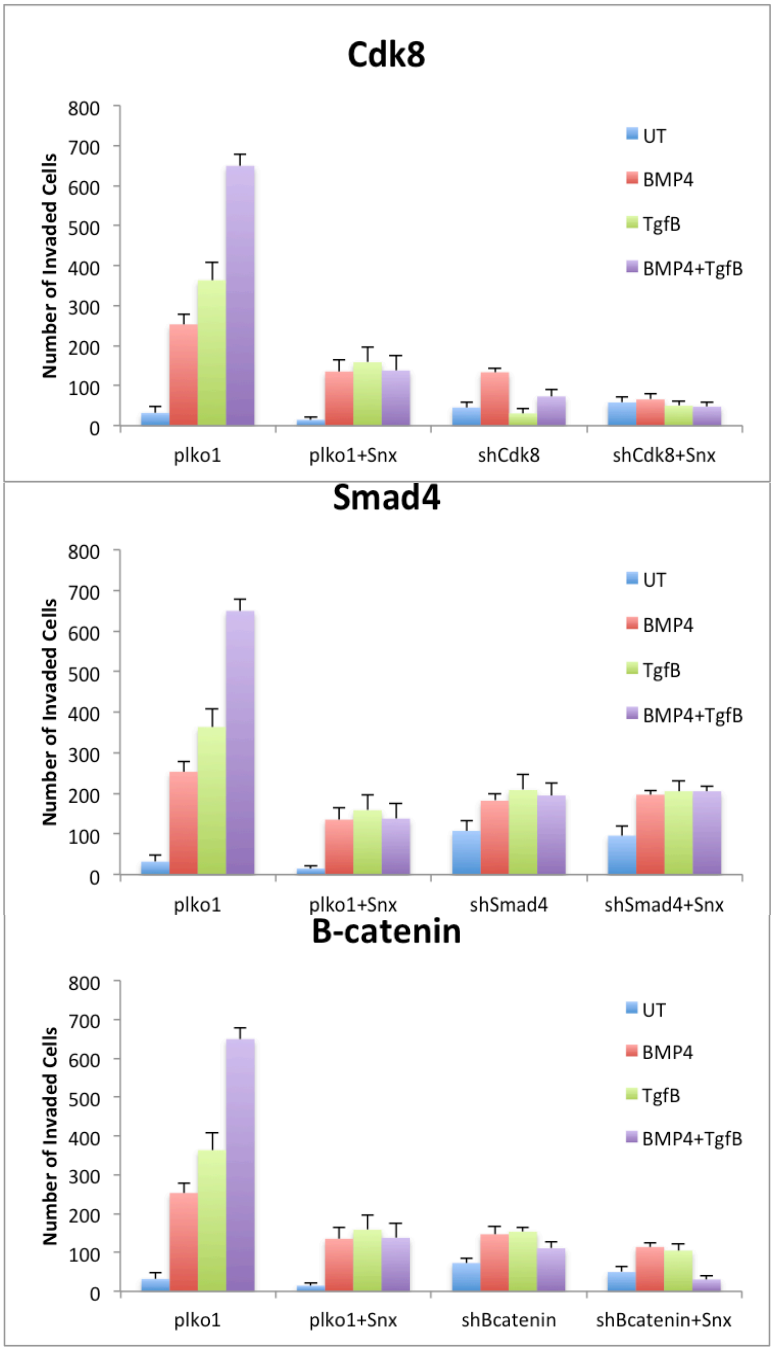


Figure C.6: Effects of SnxB, shCdk8, shSmad4, & shB-catenin on Invasion 3. shCdk8 (A), shSmad4 (B), and shBcatenin (C) on BMP4 Induced EMT. Expt S-32.

**Appendix D**
**Py2T Data**

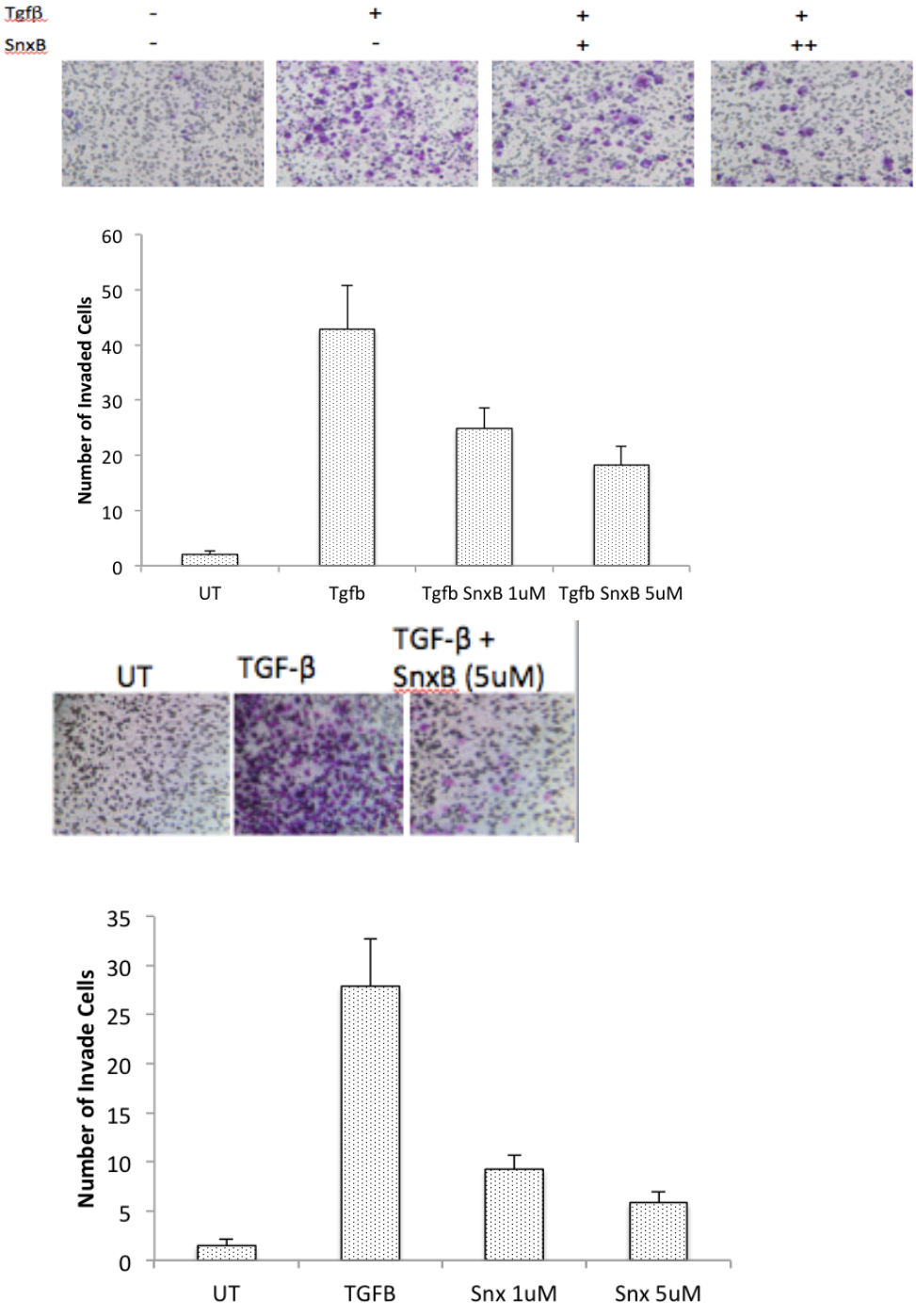


Figure D.1: Effects of SnxB on Tgf-β1 Induced Invasion. Expt. S-18.

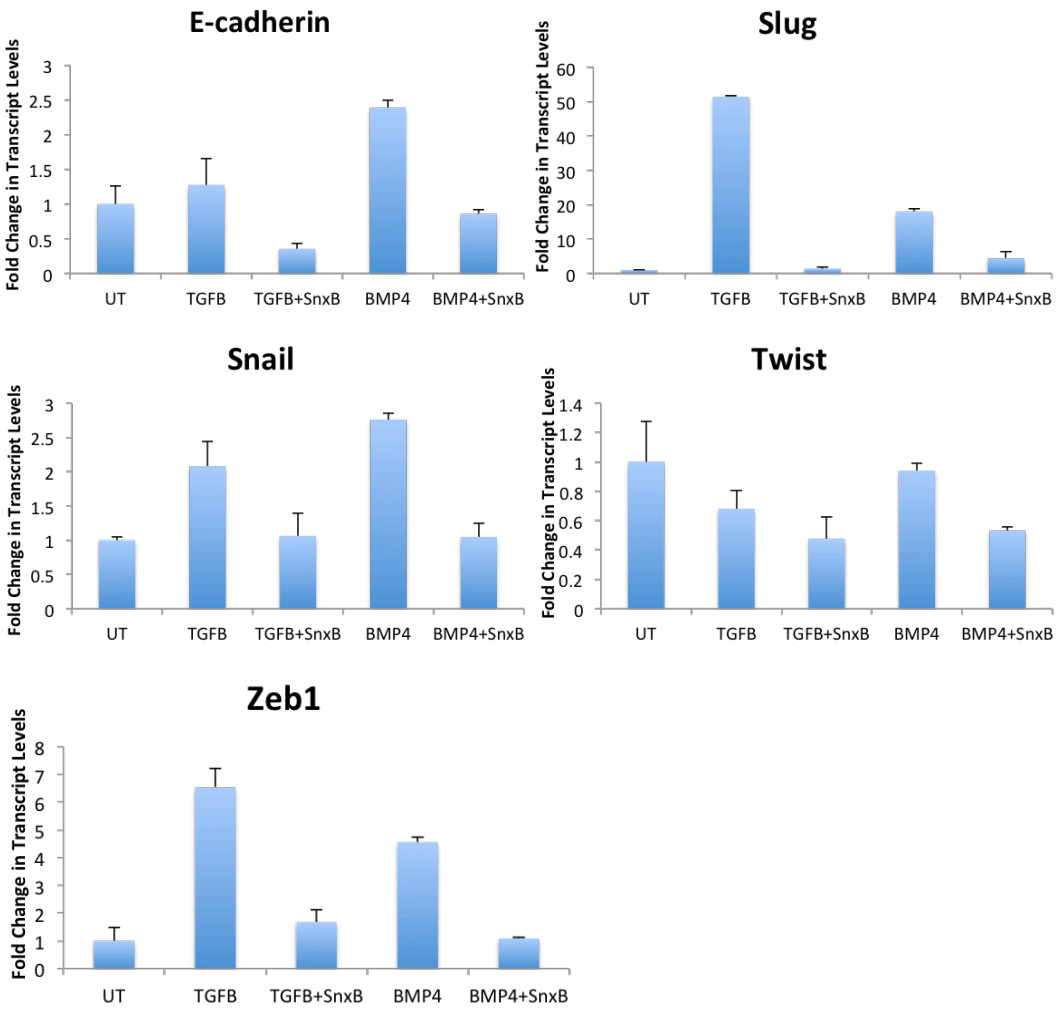


Figure D.2: Effects of SnxB on Tgf–β1 and BMP4 Induced EMT. Expt. 2-34.

**Appendix E**
**Miscellaneous Data**

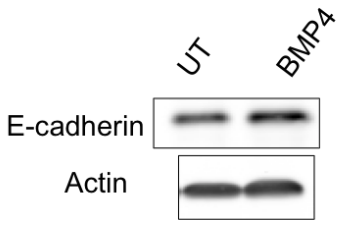


Figure E.1: Effects of BMP4 on EMT in OvCa4 Cells

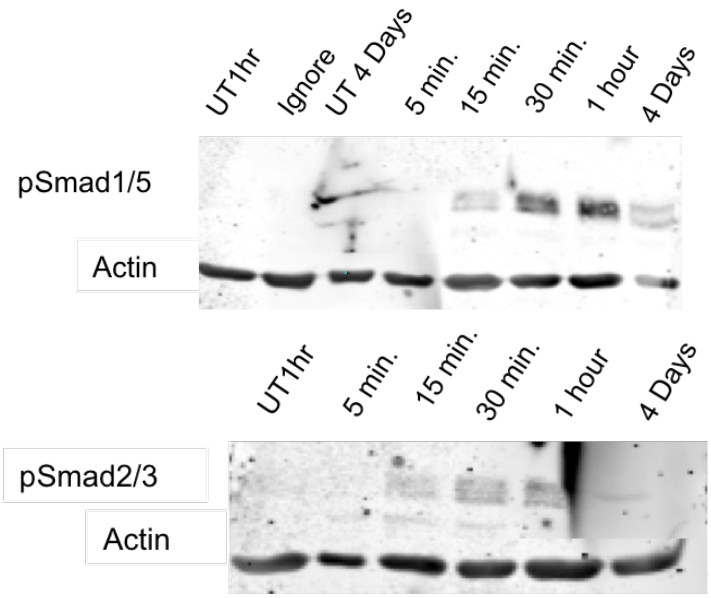


Figure E.2: Effects of BMP4 on Smad Signaling in OvCa433 Cells.

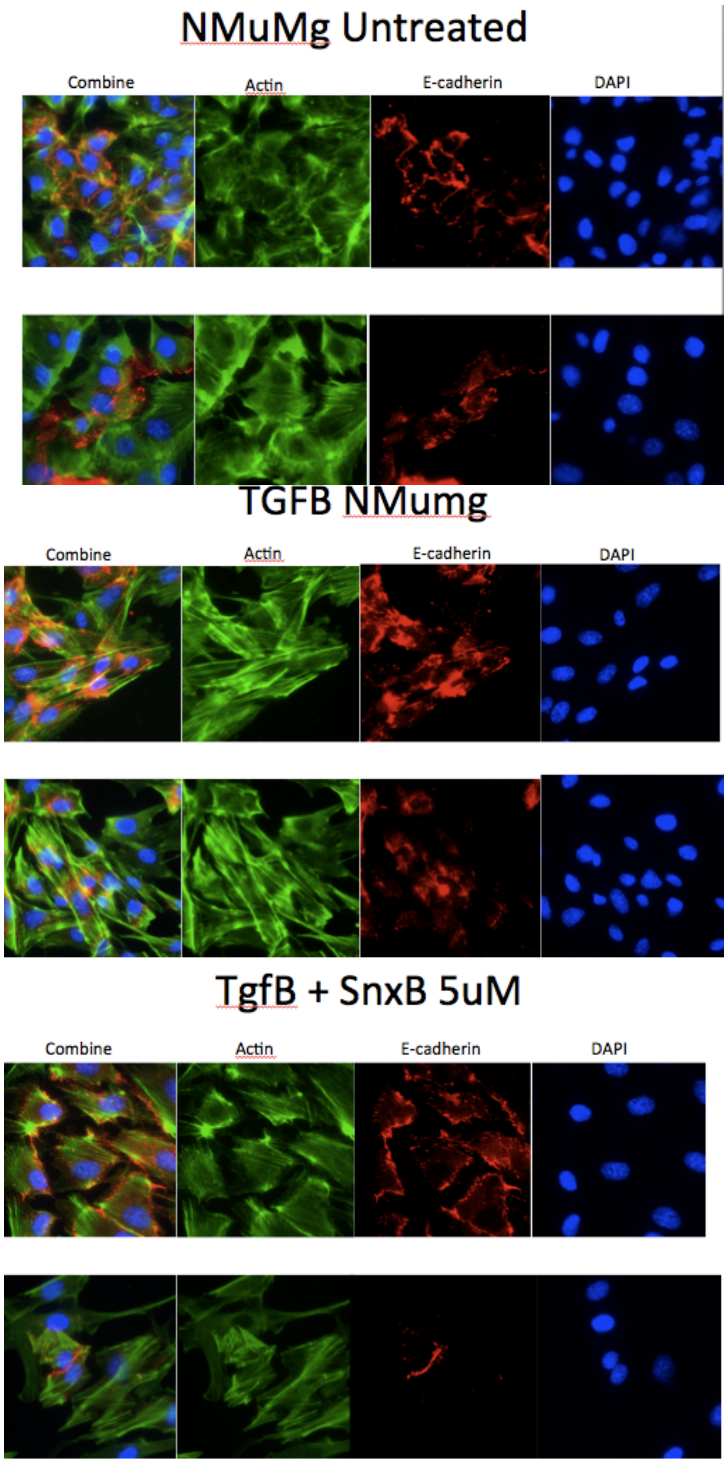


Figure E.3: Effects of SnxB on Tgf-β Induced EMT in NMuMg Cells.

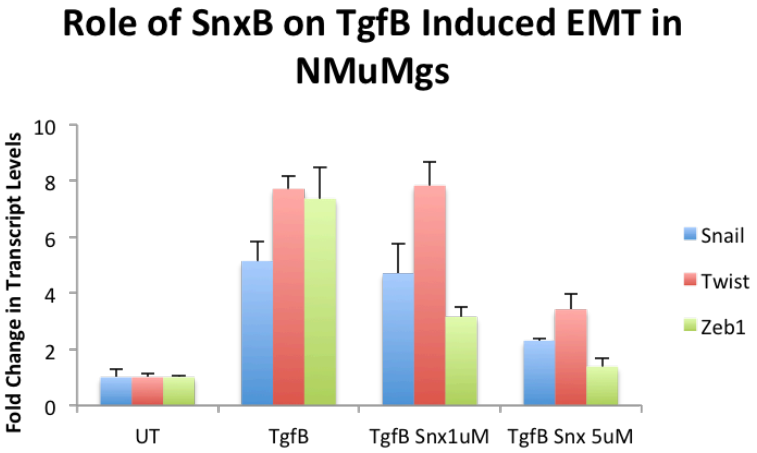


Figure E.4: Effects of SnxB on Tgf-β Induced EMT in NMuMg Cells. Expt S-11.

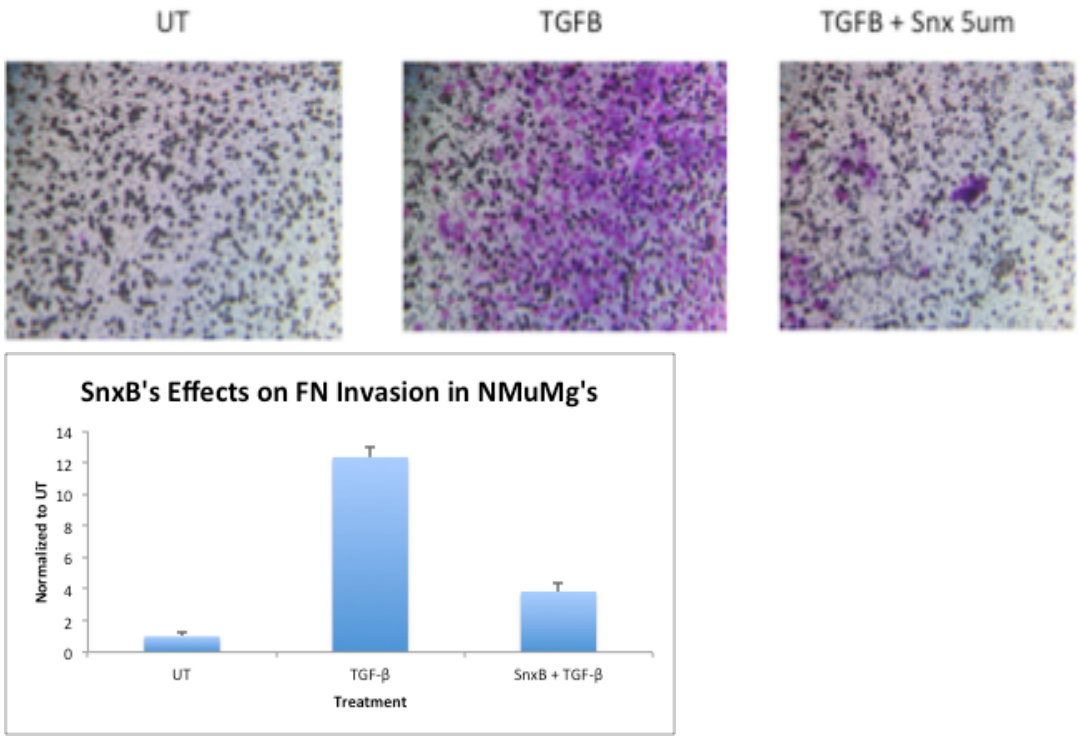


Figure E.5: Effects of SnxB on Tgf-β Induced FN Invasion in NMuMg Cells. Expt. S-17.